Life-Cycle analysis of economic and environmental effects for electric bus transit systems

Transportation Research Part D 131 (2024) 104205

Contents lists available at ScienceDirect

Transportation Research Part D

journal homepage: www.elsevier.com/locate/trd

Life-Cycle analysis of economic and environmental effects for electric bus transit systems

Mingyang Pei [a], Yi Hu [a], Weiji Han [b,*], Xiaobo Qu [c], Changfu Zou [d,*]

[a] School of Civil Engineering & Transportation, South China University of Technology, Guangzhou 510640, China
[b] China-UK Low Carbon College, Shanghai Jiao Tong University, Shanghai 201306, China
[c] School of Vehicle and Mobility, Tsinghua University, Beijing 100084, China
[d] Department of Electrical Engineering, Chalmers University of Technology, Gothenburg SE-412 96, Sweden

ARTICLE INFO

Keywords:
Electric buses
Charging systems
Life-cycle cost
Environmental effect
Optimization
Battery degradation

ABSTRACT

Electric buses play a crucial role in reducing the carbon footprint. This study evaluates the life cycle costs (LCCs) and environmental impacts of three e-bus transit systems: stationary charging, battery swapping, and dynamic wireless charging. A mixed-integer nonlinear optimization problem is formulated to determine the optimal design parameters for the charging infrastructure, bus fleet size, and battery capacity for each e-bus transit system considering battery degradation. Taking Guangzhou's Bus Rapid Transit (BRT) system as an example, a sensitivity analysis of the optimized solution is conducted. The LCC analysis framework is extended to BRT systems in 38 cities globally. The results indicate the superiority of battery swapping in most cases, while stationary charging and dynamic wireless charging are more competitive in cases with long circuit lengths and high service frequencies. Dynamic wireless charging becomes the best option when charging infrastructure is shared with other bus lines or private cars.

1. Introduction

Modern transportation relies heavily on fossil fuels and has become the leading cause of energy consumption, air pollution, and climate change (An et al., 2020; Manzolli et al., 2022; Ruan and Lv, 2022). For example, in Europe, approximately 25 % of greenhouse gas (GHG) emissions are generated by transportation systems (European Environment Agency, 2020). Therefore, there is a global urgency to develop a sustainable transportation system. Featuring high energy efficiency and environmental friendliness, transportation electrification enabled by rechargeable batteries has been widely recognized as an effective solution to the above problems of conventional transport (Bi et al., 2016; Chatzikomis et al., 2014; Qu and Wang, 2021; Shi et al., 2021; Wang et al., 2022a; Zhou et al., 2022). In this context, the European Union has made a visionary commitment to achieve 55 % of zero-emission vehicles among all vehicles by 2030 (European Commission, 2021). China has also promised to reach at least a 20 % market share for purely electrified transport by 2025, with plans to fully electrify all buses by 2035 and ultimately achieve carbon neutrality by 2060 (KPMG, 2021). The United States recently announced a $174 billion investment to boost the production and sale of zero-emission transport (Department of Transportation, 2021). To accomplish these goals, electric bus (e-bus) transit systems are key players in creating road maps for transportation electrification (Ji et al., 2022; Liu et al., 2022; Zhang et al., 2023).

* Corresponding authors.
E-mail addresses: mingyang@scut.edu.cn (M. Pei), cthuyi@mail.scut.edu.cn (Y. Hu), w.han@sjtu.edu.cn (W. Han), xiaobo@tsinghua.edu.cn (X. Qu), changfu.zou@chalmers.se (C. Zou).

https://doi.org/10.1016/j.trd.2024.104205
Received 4 August 2023; Received in revised form 4 January 2024; Accepted 11 April 2024
Available online 23 April 2024

An e-bus transit system commonly consists of charging infrastructure, electric buses, and batteries. Such a system incurs sizeable capital costs and has a considerable impact on the environment (Zhang et al., 2022). The initial construction cost for charging infrastructure can range from $300,000 to $500,000, depending mainly on the construction area and the number of chargers (Bi et al., 2017). According to a financial analysis conducted by the National Renewable Energy Laboratory in 2020 (Johnson, 2020), the purchase cost for an e-bus was approximately $887,308, which is $480,000 higher than the price of a conventional diesel bus. While the unit price for batteries has gradually decreased, it was still approximately $273/kWh for 2020 in Sweden (Statista Research Department, 2021). Therefore, minimizing these capital costs to improve the cost competitiveness of the whole system is an important consideration. On the other hand, the growing number of e-buses, especially those powered by renewable energy (Nordelöf et al., 2019), can contribute to emission reduction (Borén, 2020). In addition to e-buses, the environmental impacts of constructing charging infrastructure and manufacturing batteries need to be considered. Thus, designing a cost-effective and sustainable e-bus transit system is highly important.

With advances in battery research and development as well as associated charging techniques, e-bus charging infrastructure has made substantial progress (Fuller, 2016; He et al., 2020; Jang, 2018; Olsen and Kliewer, 2022; Wang et al., 2022a; Zeng and Qu, 2023; Zhou et al., 2022) over the past decade. Some e-bus charging infrastructures are summarized in Fig. 1, including terminal charging stations, depot charging stations, opportunity charging stations (e.g., based on pantograph chargers or wireless charging pads), battery swapping stations, wireless charging lanes, etc. These are deployed in three typical e-bus charging solutions: stationary charging, swapping charging, and charging in motion. In stationary charging (see Fig. 1(a)–(d)), buses are charged when parked at a depot or bus station along the bus route, which is preferred by many e-bus companies (Ke et al., 2016; Statusrapport, 2020; Zheng et al., 2014). Specifically, stationary charging at a terminal (see Fig. 1(a)) or a bus depot (see Fig. 1(b)) can provide long-term charging services for a large bus fleet. If e-buses are allowed to be charged at intermediate bus stations, such a stationary charging solution is called opportunity charging (Andersson, 2017), which can be implemented using pantograph chargers, as shown in Fig. 1(c) (Lehmann, 2021), or through stationary wireless power transfer (WPT), as shown in Fig. 1(d) (Panchal et al., 2018). A battery swapping solution entailing swapping stations and spare batteries, as shown in Fig. 1(e), allows exhausted batteries to be replaced with fully charged batteries and provides a centralized battery charging service (Zhong and Pei, 2020). Thus, this solution features a very short service time for e-buses. In addition, a solution for charging while in motion was developed using WPT technology, and it supports electrical power transmission without wires based on time-varying electric, magnetic, or electromagnetic fields (Majhi et al., 2021). While the investment in this solution is extremely high, as shown in Fig. 1(f), dynamic wireless charging lanes (DWCLs) equipped with WPT facilities (such as magnetic coils) and supported by a power grid can provide continuous charging services for running buses (Fuller, 2016; He et al., 2013, 2020; Jang, 2018; Kim et al., 2019; Pei et al., 2023; Liang and Chowdhury, 2018).

These e-bus charging solutions and associated infrastructures are further compared in Table 1 based on suitable scenarios, applications, and typical features. Each e-bus charging solution has unique advantages and limitations. Depending on the practical application scenario, these charging solutions can be either individually deployed or combined.

Several recent studies have analyzed the cost competitiveness of e-bus transit systems with different charging solutions from economic and environmental perspectives, as compared in Table 2. Various cost components of the deployed charging infrastructure,

Fig. 1. Typical e-bus charging infrastructures. (a) Terminal charging station allowing overnight parking and charging (ABB Group, 2021). (b) Depot charging station with plug-in chargers (Co, 2021). (c) Opportunity charging station equipped with pantograph chargers (Lehmann, 2021). (d) Opportunity charging station with a stationary wireless charging pad (Lambert, 2018). (e) Battery swapping station (XJ Group Corporation, 2021). (f) Dynamic wireless charging lane (Chesky, 2021).

Table 1
Comparison of prevailing e-bus charging solutions and associated infrastructures.

Charging solution	Charging infrastructure		Charging within a service circuit	Suitable scenarios	Application/testing	Features	Reference
Stationary charging	Terminal charging station Fig. 1(a) and (b)		No	Long charging time, e.g., overnight at end terminals	Used by most e-bus companies, e.g., 8 ABB e-bus chargers for 411 e-buses in operation in Chile	Cutting costs or electricity consumption; slow end-terminal charging is suitable for shorter routes	(Andersson, 2017; Charging, 2010; Lajunen, 2018)
	Opportunity charging station	Plug-in Fig. 1(c)	Yes	Longer routes and smaller battery size	Cities in China; Gothenburg, Sweden	Allows decentralized overnight charging scheduling; more charging points leading to shorter end-terminal charging times and a decreased e-bus fleet size	(Bi et al., 2017, 2015; Ke et al., 2016)
		Wireless Fig. 1(d)	Yes		Tested by some research groups		(Bi et al., 2015; Jang et al., 2016; Mohamed et al., 2020)
Swapping charging	Battery swapping station Fig. 1(e)		No	Replicating the experience at existing gas stations	Battery exchange stations implemented in Israel and Denmark by Better Place (company)	Decreases the e-bus fleet size; provides fast and economical charging systems	(Adler and Mirchandani, 2014; Mak et al., 2013; Yang et al., 2014)
Charging in motion	Dynamic wireless charging lane (DWCL) Fig. 1(f)		Yes	Eliminating the waiting time at recharge stations	Online electric vehicles (OLEVs) developed by KAIST	Allows charging while moving; minimal battery size; designed for use on heavy-load traffic corridors/freeways	(Bi et al., 2019; Chen et al., 2017; He et al., 2020; Jang, 2018; Liu and Song, 2017; Suomalainen and Colet, 2019)

e-buses, and batteries need to be considered in the analysis of each e-bus transit system. In particular, the environmental effect can be quantified in terms of the GHG emission cost (Bi et al., 2019, 2017; García et al., 2022). While these cost components were analyzed partially in recent studies, this work accounts for all of these cost components in a comprehensive life-cycle cost (LCC) analysis for each type of e-bus transit system. The LCC of an e-bus transit system covers all costs throughout the system lifespan, e.g., the sum of the initial investment, recurring costs, and future additional investments minus any salvage value (Jagdishsingh and S Patil, 2014). The obtained quantitative results provide effective guidelines and references for the appropriate design of e-bus transit systems in various cities.

As shown in Table 2, while several researchers (Bi et al., 2019; Lajunen, 2018; Zhang et al., 2021) have investigated one specific e-bus transit system, multiple e-bus transit systems have been jointly analyzed in other studies (Bi et al., 2017; Chen et al., 2018; Wang et al., 2022b). However, in all these recent studies, each e-bus transit system was equipped with only one type of charging infrastructure, as listed in Table 1, which inevitably limited the exploration and exploitation of the combined merits of different charging solutions, as well as their synergetic effects. Furthermore, there has been no unified and systematic optimization study covering all the involved design parameters relating to infrastructure construction, bus purchases, battery replacement, and GHG emissions over their life cycles. This means that state-of-the-art methods yield inferior solutions or local minima. For example, the battery capacity fades over charge and discharge cycles, resulting in declining e-bus performance. Thus, it is highly important to consider battery degradation in the parameter design and LCC analysis stages of e-bus transit systems.

This work aims to bridge the identified research gaps from several important aspects. Three types of e-bus transit systems are investigated, and two different charging solutions can be combined to achieve the optimal result. Then, for each e-bus transit system, an LCC optimization framework for economic costs and environmental effects is developed, and a mixed-integer nonlinear optimization problem is formulated to determine the best design parameters for the charging infrastructure, bus fleet, and battery systems and to explicitly consider battery capacity degradation and salvage values. Moreover, a comprehensive sensitivity analysis is conducted to quantitatively identify the key factors affecting the life cycle performance and cost of various e-bus transit systems. Finally, the developed framework and sensitivity analysis method are applied to BRT in 38 cities across different countries. The obtained results can be used to facilitate the optimal planning and operation of e-bus transit systems

2. E-bus transit systems investigated in this work

Three types of e-bus transit systems, as illustrated in Fig. 2, are investigated, encompassing all the common e-bus charging solutions summarized in Table 1. Since end-terminal charging can provide efficient energy transfer due to a low charging rate (Liu and (Avi) Ceder, 2020) and help decrease the heavy load on the power grid (Lukic and Pantic, 2013), this approach has already been combined

Table 2
Comparison of cost analyses of previous e-bus transit systems and that in this work.

		(Bi et al., 2017)	(Chen et al., 2018)	(Lajunen, 2018)	(Bi et al., 2019)	(Zhang et al., 2021)	This work
Charging infrastructure	End terminal charging	√	√	√	–	–	√
	Opportunity charging	–	–	–	–	–	√
	Battery swapping	–	√	–	–	√	√
	Dynamic wireless charging lanes	√	√	–	√	–	√
	Joint charging infrastructure	–	–	–	–	–	√
Cost components	Life cycle cost analysis	√	–	√	√	√	√
	Infrastructure construction cost	√	√	√	√	√	√
	Bus purchase cost	√	–	–	–	√	√
	Battery purchase cost	√	√	√	–	√	√
	Operating cost	√	–	√	–	–	√
	Battery salvage value	√	√	√	–	–	√
	Battery replacement cost	–	–	√	–	√	√
	Bus replacement cost	–	–	√	–	√	√
	Greenhouse gas emission cost	√	–	–	√	–	√
Design parameter optimization	Charging infrastructure Deployment	–	√	–	√	–	√
	Bus fleet size	–	√	–	–	–	√
	Number of batteries	–	√	–	–	–	√
	Battery capacity size	–	√	–	–	√	√
	Operating route	–	–	√	–	–	–
	Charging method	–	√	√	–	–	√
	Charging time or scheduling	–	–	–	–	√	√
	Battery replacement period	–	–	–	–	–	√
	The year to deploy charging lanes	–	–	–	√	–	–
Other features	Battery degradation	–	–	–	–	√	√
	Battery replacement period	12 years	12 years	12 years	–	Flexible	Flexible

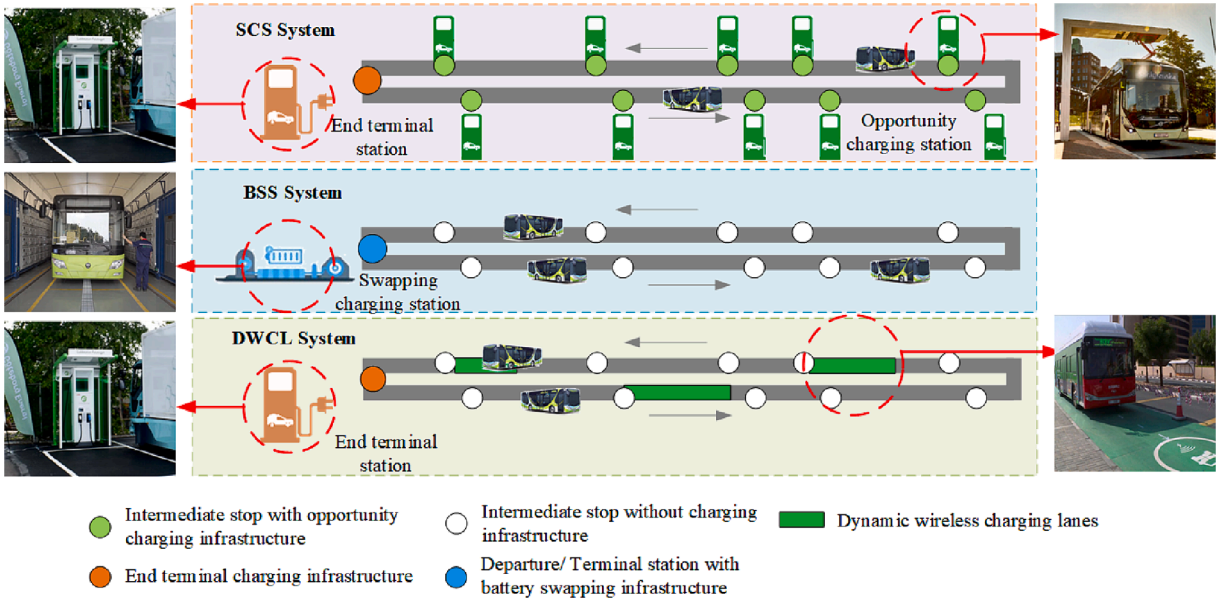

Fig. 2. E-bus transit systems investigated in this work.

with opportunity charging in real-world e-bus transit systems in Sweden and is integrated into DWCL charging in this work.

The e-bus transit system of bus lines 55 and 16 in Gothenburg, Sweden, as described at the top of Fig. 2, is referred to as a stationary charging station (SCS) system since buses can be charged either at end-terminal charging stations or opportunity charging stations, with pantograph chargers located at certain bus stops (Lehmann, 2021). When an e-bus arrives at an opportunity charging station, its charging time equals the bus dwelling time at the stop minus the time needed to connect/disconnect the charger.

The second e-bus transit system to be investigated is the battery swapping station (BSS) system, as shown in the middle of Fig. 2. This system allows an e-bus to replace its exhausted battery with a fully charged battery at a BSS, which are commonly located at bus depots with sufficient space or end-terminal stations. After a swap, buses are equipped with fully charged batteries, and the number of travel circuits before the next swap can be optimized. The BSS system can support quick battery swapping services (regarded as ultrafast charging) and, hence, can be used to downsize the required e-bus fleet. Moreover, an exhausted battery can be fully charged at a swapping station, and such centralized charging can be used to improve power grid operation, e.g., peak shaving.

Another e-bus transit system is the DWCL system, which involves both wireless charging lanes and terminal charging stations, as demonstrated at the bottom of Fig. 2. Buses can be charged sufficiently overnight at a terminal charging station, commonly with low electricity costs and high power transfer efficiency. When driving along a route, buses can also be charged via enroute wireless charging lanes without slowing. As a result of both in-motion and end-terminal charging, it is possible to largely downsize the capacity of e-bus batteries. These three e-bus transit systems are further compared in Table 3 in terms of their strengths, weaknesses, and application scenarios.

Table 3
Summary of three e-bus transit systems.

	SCS system	BSS system	DWCL system
End-terminal charging	√		√
Opportunity charging	√		
Battery swapping		√	
Dynamic wireless charging lanes			√
Strengths	High energy transfer efficiency and supports grid-level ancillary services (end-terminal charging); Downsized battery capacity (opportunity charging)	Short service time, lower construction cost than SCS systems, and centralized charging	High energy transfer efficiency and supports grid-level ancillary services (end-terminal charging); Charging in motion and downsized battery capacity (DWCLs)
Weaknesses	High construction cost and requires a large land area	Large battery purchase cost	Very high construction cost and low energy transfer efficiency
Application scenarios	Long and heavy-volume traffic corridors (opportunity charging)	Short e-bus circuits with light traffic volume	Long and heavy-volume traffic corridors

3. Problem description and formulation

3.1. Notations and assumptions

To characterize the three types of e-bus transit systems in Fig. 2 and analyze their LCC competitiveness, all the notations used throughout this study are listed and defined in Table 4.

To facilitate the modeling of the three investigated e-bus transit systems, the following assumptions are introduced.

Table 4
Nomenclature.

Sets			
$\mathscr{I}$	Set of bus stops ,$\mathscr{I} := \{1, 2, \cdots, I\}$	$\mathscr{K}$	Set of service circuits for a day of operation ,$\mathscr{K} := \{1, 2, \cdots, K\}$
$\mathscr{J}$	Set of LCC analysis years,$\mathscr{J} := \{1, 2, \cdots, J\}$		
Parameters			
i	Index of the intermediate bus stops, $i \in \mathscr{I}$; $i = 0$ denotes an end-terminal charging station	j	Index of the LCC analysis year,$j \in \mathscr{J}$
f	Service frequency, circuits per hour	T	Hours of bus operation per day, h/day
$N_{day,j}$	Average days of operation in year j	v	Average bus speed
t_{stop}	Average stop time for alighting and boarding, h	$t_{c,s}$	Maximum charging time for an exhausted battery at a BSS, h
$t_{c,o}$	Charging time at an opportunity charging station, h	t_{swap}	Time to swap out a battery, h
τ_L	Estimated lifetime for the system, years	l_i	Route distance from stop $i-1$ to stop i, $i \in \mathscr{I}$
C_β	Monetary value of emissions	$l_{year,j}$	Cumulative distance driven by all buses in year j
a_{WTT}	Monetary global warming impact based on the well-to-tank (WTT) system	d_{rate}	Annual discount rate
τ_{BUS}	Mandatory scrap life of e-buses	a_{ELC}	Monetary global warming impact based on the equipment life cycle (ELC)
SoC_{avg}	Average SoC for a single charge processed	SoC	E-bus battery state of charge (SoC), with the range $[SoC_{min}, SoC_{max}]$, %
ξ	Capacity fading rate	$\mathrm{SoC}_{\mathrm{dev}}$	Normalized standard deviation from SoC_{avg}
$P_{c,o}$	Charging power for an opportunity charging station	SoH_j	Battery state of health in year j
$P_{c,end}$	Charging power for an end-terminal charging station	EoL	Battery end of life
$P_{c,s}$	Charging power for a swapping station, W	E_d	Battery energy consumption per km (kWh/km)
$E_{c,l}$	Battery energy charged per km on a DWCL, kWh/km	$V_{c,s}$	Average charging voltage for the BSS charging mode, V
$V_{c,o}$	Average charging voltage for an opportunity charging station, V	$V_{c,l}$	Average charging voltage for dynamic lane charging, V
$V_{c,end}$	Average charging voltage for an end-terminal charging station, V	$C_{m,bus}$	Annual maintenance cost of an e-bus
V_d	Average discharging voltage, V	F_{OP}	Operating cost
F_{LCC}	Life cycle cost	F_{GG}	Greenhouse gas emission cost
F_{CAP}	Capital cost	F_{REP}	Technology replacement cost
F_{CO}	Construction cost	$F_{energy,j}$	Energy consumption cost in year j
F_{BUS}	Initial bus purchase cost	$F_{maint.,j}$	Maintenance cost in year j
F_{BA}	Initial battery purchase cost	$C_{m,ba}$	Unit maintenance cost for a battery
$C_{m,infra.}$	Charging infrastructure maintenance cost	$C_{m,bus}$	Unit maintenance cost for an e-bus
C_{BA}	Unit battery purchase cost per kWh	C_{BUS}	Initial bus purchase cost
C_{SV_BA}	Unit salvage value of bus batteries per kWh	C_{SV_BUS}	Unit salvage value of a bus
C_{GG}	Unit greenhouse gas cost	$C_{c,t}$	Construction cost for the inverter in a DWCL
F_{R_BA}	Battery technology replacement cost	$C_{c,l}$	Unit construction cost for a DWCL per km
F_{R_BUS}	Bus replacement cost	$C_{p,end}$	Unit energy cost for end-terminal charging stations per kWh
C_{end}	Construction cost for one end-terminal charging station	$C_{p,o}$	Unit energy cost for opportunity charging stations per kWh
$C_{c,o}$	Construction cost for one opportunity charging station	$C_{p,s}$	Unit energy cost for BSSs per kWh
$C_{c,s}$	Construction cost for one BSS	$C_{p,l}$	Unit energy cost for a DWCL per km
α_{end}	Charging efficiency for end-terminal charging	$\alpha_{c,s}$	Charging efficiency for swapped battery charging
$\alpha_{c,o}$	Charging efficiency for opportunity charging	$\alpha_{c,l}$	Charging efficiency for a DWCL
k_{s1}	Coefficient in the battery capacity fading model	k_{s3}	Coefficient in the battery capacity fading model
k_{s2}	Coefficient in the battery capacity fading model	k_{s4}	Coefficient in the battery capacity fading model
Variables			
x_i	Binary variable $x_i \in \{0, 1\}$, where $x_i = 1$ if bus stop i is chosen to provide opportunity charging	ω_j	Binary variable $\omega_j \in \{0, 1\}$, where $\omega_j = 1$ if a bus battery is replaced in year j
y_k	Binary variable $y_k \in \{0, 1\}$ denoting whether the battery is swapped at circuit k	n_{BA}	Minimum number of batteries at a BSS,$n_{BA} \in \mathbb{R}$
z_i	Binary variable $z_i \in \{0, 1\}$ denoting whether the route from bus stop $i-1$ to stop i has a charging lane	E	Initial battery size or energy capacity, kWh,$E \in \mathbb{R}$
d_i	The length of the charging lane between bus stop $i-1$ and stop i, $d_i \in \mathbb{R}$	Q	Size of the bus fleet, i.e., the number of buses in the fleet,$Q \in \mathbb{R}$

Note: All costs are presented in US dollars (USD, denoted as $ for simplicity).

Assumption 1. *All the e-buses have the same battery size and share the same initial SoH, i.e.*, 100 % *for new e-bus batteries*.

This assumption is used to calculate the battery SoC during charging/discharging and the battery SoH for battery replacement. A fully charged bus can serve at least one circuit. It must be acknowledged that in real-world scenarios, electric bus fleets may comprise buses with varying battery capacities, and the initial SoH of new batteries may exhibit some variations. However, for the intricate charging solutions and resource allocation planning issues throughout the entire lifecycle in this study, this assumption regarding the battery size and initial SoH is both acceptable, and it has been commonly employed (e.g., by Bi et al., 2019; Chen et al., 2018).

Assumption 2. *An e-bus is fully charged when starting a circuit from the end-terminal charging station or when departing a swapping station. Moreover, when an e-bus arrives at an opportunity charging station, the charging time equals the bus dwelling time at the stop*.

Considering an e-bus transit system with a fleet of homogeneous e-buses for daily transient transport service, each bus transit circuit is characterized by a round trip, as shown in Fig. 2, along which bus stops are denoted by $i \in \mathscr{I}$. The e-bus service frequency f describes the number of circuits per hour. The number of buses in the fleet, i.e., the bus fleet size, is denoted by Q. Let E denote the energy capacity or size of the bus battery system. The end of life (EoL) of an e-bus battery is reached when the battery capacity degrades to 70–80 % of its initial capacity, and we use 70 % as the EoL of the battery (Zhang et al., 2021). A bus battery needs to be replaced once its state of health (SoH) reaches EoL. Let the binary variable ω_j denote whether a bus battery is replaced in year j, and let $\omega_j = 1$ indicate the battery replacement.

Assumption 3. *The electric energy consumption of e-buses is assumed to be proportional to the driving distance*.

Since e-buses are repeatedly running along a fixed circuit, an e-bus's overall energy consumption for each circuit does not change significantly. This can be obtained from practical e-bus driving data or simulation tests. Then, the average energy consumption per kilometer can be obtained, as specified by the parameter E_d, and the e-bus's energy consumption is dependent mainly on driving distance. Similar assumptions were also made in related studies (Lajunen, 2018; Zhang et al., 2021). Notably, the above assumption based on E_d is suitable for estimating the total energy consumption across circuits, but the accuracy might be compromised when estimating the real-time consumption within one circuit. During practical operation of e-buses, real-time energy consumption is influenced not only by the driving distance but also by the driving speed, acceleration/deceleration behaviors, environmental temperature, rolling resistance, aerodynamic drag, etc.

For an SCS system, if bus stop i is selected to provide opportunity charging, the binary variable x_i is set to 1. Moreover, for a BSS system, if the bus battery is swapped at circuit $k \in \mathscr{K}$, the binary variable y_k is set to 1. Let the variable n_{BA} denote the minimum number of batteries in the BSS. If a BSS has sufficient spare batteries, a quick battery swapping service can be provided. In addition, for the DWCL system, the binary variable z_i is set to 1 if there exists a charging lane between bus stop $i-1$ and stop i, and the length of this charging lane is denoted by d_i.

3.2. Life cycle costs

The LCC analysis seeks to optimize the cost of acquiring, owning, and operating physical assets over their useful lives by identifying and quantifying all the significant costs involved using the present value technique (Woodward, 1997). In this work, the costs incurred in the LCC analysis of an e-bus transit system consist of the initial investment (i.e., initial capital cost), future additional investments (i.e., replacement costs of batteries and buses), and annually recurring costs (i.e., operating cost and GHG emission cost).

Given one type of e-bus transit system, e.g., an SCS, a BSS, or a DWCL system, the LCC is denoted by F_{LCC} and calculated as follows:

$$F_{LCC} = F_{CAP} + F_{OP} + F_{GHG} + F_{REP}, \tag{1}$$

where F_{CAP} denotes the initial capital cost, F_{OP} is the operating cost, F_{GG} is the GHG emission cost, and F_{REP} is the technology replacement cost.

3.2.1. Initial capital cost

The initial capital cost F_{CAP} mainly includes the initial construction cost of the deployed charging infrastructure F_{CO}, the initial purchase cost of e-buses F_{BUS}, and the initial purchase cost of batteries F_{BA} and is modeled by

$$F_{CAP} = F_{CO} + F_{BUS} + F_{BA}. \tag{2}$$

The initial construction cost F_{CO} varies significantly depending on the deployed charging infrastructure. For the SCS system in Fig. 2, F_{CO} includes the construction costs of the end-terminal charging station and opportunity charging stations. Let C_{end} and $C_{c,o}$ denote the unit construction costs for an end-terminal charging station and opportunity charging station, respectively. Then, the initial construction cost of one SCS is $F_{CO\_SCS} = C_{end} + C_{c,o}\sum_{i\in\mathscr{I}} x_i$, which is linearly dependent on the number of opportunity charging stations, i.e., $\sum_{i\in\mathscr{I}} x_i$. The initial construction cost of a BSS is denoted by $C_{c,s}$. The initial construction cost for the DWCL system in Fig. 2 consists of the cost of the terminal charging station, i.e., C_{end}, and the cost of the DWCLs. The first part of the DWCL cost is the construction cost of all segments, including the costs of inverters and power transmitters. The second part of the DWCL cost is the construction cost of wireless electric lanes, underground feeders, and pavement. Let $C_{c,t}$ and $C_{c,l}$ denote the initial construction cost of each segment and each kilometer of charging lane, respectively. The initial construction cost of the DWCL can be described as $F_{CO\_DWCL} = C_{end} + \sum_{i\in\mathscr{I}} C_{c,t} z_i + \sum_{i\in\mathscr{I}} C_{c,l} d_i$. The unit construction cost for each charging infrastructure is extracted from Chen et al.

(2018), as detailed in Table 7. In this study, these unit construction costs are assumed to be independent of location and capacity. The initial construction cost of each type of e-bus transit system in Fig. 2 is summarized as follows:

$$F_{CO} = \begin{cases} C_{end} + C_{c,o}\sum_{i\in\mathscr{I}} x_i, & \text{for an SCS system,} \\ C_{c,s}, & \text{for a BSS system,} \\ C_{end} + \sum_{i\in\mathscr{I}} C_{c,l} z_i + \sum_{i\in\mathscr{I}} C_{c,l} d_i, & \text{for a DWCL system.} \end{cases} \tag{3}$$

The initial bus purchase cost F_{BUS} is

$$F_{BUS} = C_{BUS} Q, \tag{4}$$

where C_{BUS} denotes the price of each bus.

The initial battery purchase cost F_{BA} can be calculated based on the battery unit price per kWh C_{BA}, the battery energy capacity E of each bus, and the number of batteries n_{BA}, as summarized in (5). In the SCS and DWCL systems, the number of batteries n_{BA} is equal to the number of buses in the fleet, i.e., the fleet size Q. The BSS entails spare batteries for rotation, so the number of batteries n_{BA} in a BSS system is larger than the fleet size Q. The battery energy capacity E and the number of bus batteries (i.e., n_{BA} or Q) are viewed as decision variables in the optimization problem.

$$F_{BA} = \begin{cases} C_{BA} E Q, & \text{for an SCS system or a DWCL system,} \\ C_{BA} E n_{BA}, & \text{for a BSS system.} \end{cases} \tag{5}$$

3.2.2. Operating cost

For an e-bus transit system, the total operating cost throughout the life cycle F_{OP} consists of two parts, namely, the energy consumption cost, $F_{energy,j}$ for year j, and the maintenance cost, $F_{maint.,j}$ for year j. Then, based on the annual recurring costs, F_{OP} is calculated by

$$F_{OP} = \sum_{j=1}^{\tau_L} \left(F_{energy,j} + F_{maint.,j}\right)(1 + d_{rate})^{-j}, \tag{6}$$

where d_{rate} denotes the discount rate and τ_L is the estimated lifetime of the entire system in years. The yearly energy consumption cost $F_{energy,j}$, measured in kWh, can fluctuate over time and can be calculated for each type of e-bus transit system as follows:

$$F_{energy,j} = \begin{cases} \left(C_{p,end}(SoC_{max} - SoC_I)E \Big/ \alpha_{end} + \sum_{i\in\mathscr{I}} x_i C_{p,o} P_{c,o} t_{c,o} \Big/ \alpha_{c,o}\right) f T N_{day,j}, & \text{for an SCS system,} \\ \sum_{k\in\mathscr{K}} y_k C_{p,s}(SoC_{max} - SoC_k) Q N_{day,j} E / \alpha_{c,s}, & \text{for a BSS system,} \\ \left(C_{p,end}(SoC_{max} - SoC_I)E \Big/ \alpha_{end} + \sum_{i\in\mathscr{I}} z_i C_{p,l} E_{c,l} d_i \Big/ \alpha_{c,l}\right) f T N_{day,j}, & \text{for a DWCL system.} \end{cases} \tag{7}$$

For the SCS system shown in Fig. 2, the yearly energy consumption is equal to the energy consumed during one circuit multiplied by the total number of circuits served in one year. The latter can be obtained based on the number of circuits per hour, i.e., the service frequency f, the number of bus operation hours per day T, and the total operating days in a year $N_{day,j}$; the former can be obtained based on both end-terminal charging and opportunity charging patterns. During the end-terminal charging process, roughly assuming no battery voltage dynamics, the energy consumption is $(SOC_{max} - SOC_I)E$ divided by the energy transfer efficiency α_{end}. If a bus is charged at stop i, i.e., $x_i = 1$, the energy cost during opportunity charging can be calculated based on the corresponding electricity price $C_{p,o}$, charging power efficiency $\alpha_{c,o}$, charging power $P_{c,o}$, and charging time $t_{c,o}$, which equals the bus dwelling time t_{stop} at the stop. The electricity price and charging power efficiency can vary among different types of charging infrastructures; hence, they are separately denoted. For the BSS system, the energy consumed in year j is the sum of the energy consumed in circuit k multiplied by the bus fleet size and the total operating days. For the DWCL system in Fig. 2, the energy cost is associated with end terminal charging and the DWCL charging. The former cost is already expressed in the energy cost for the SCS system, and the latter cost can be derived from the DWCL assignment variable z_i, electricity price $C_{p,l}$, charging power efficiency $\alpha_{c,l}$, charged battery energy per km on a DWCL $E_{c,l}$, and charging lane length d_i.

The maintenance cost of e-buses and associated charging infrastructure in year j is denoted by $F_{maint.,j}$ and calculated using (8), in which the e-bus maintenance cost $C_{m,bus}$, battery maintenance cost $C_{m,ba}$, and different charging infrastructure maintenance costs ($C_{m,infra.,end}$, $C_{m,infra.,opp}$, $C_{m,infra.,BSS}$ and $C_{m,infra.length}$) are assumed to be constant. Then, $F_{maint.,j}$ mainly depends on the number of buses in fleet Q, the number of deployed batteries n_{BA}, the number of opportunity charging stations x_i and the length of the charging lane d_i.

$$F_{maint.,j} = \begin{cases} \left(C_{m,bus} + C_{m,ba}\right)Q + C_{m,infra.,end} + C_{m,infra.,opp}\sum_{i\in\mathscr{I}} x_i, & \text{for an SCS system,} \\ C_{m,bus} Q + C_{m,ba} n_{BA} + C_{m,infra.,BSS}, & \text{for a BSS system,} \\ \left(C_{m,bus} + C_{m,ba}\right)Q + C_{m,infra.,end} + C_{m,infra.length}\sum_{i\in\mathscr{I}} d_i, & \text{for a DWCL system.} \end{cases} \tag{8}$$

3.2.3. GHG cost

While the analyses of GHG costs in previous studies focused on buses, the GHG costs of charging facilities are also analyzed in this work. The GHG cost of an e-bus transit system across the LCC analysis period is characterized by

$$F_{GHG} = C_\beta \left(F_{GHG,facility} + \sum_{j=0}^{\tau_L} F_{GHG,e-bus} (1 + d_{rate})^{-j} \right), \tag{9}$$

where C_β is a monetary scalar used to convert emissions into capital costs and d_{rate} is the annual discount rate.

To calculate the life cycle GHG emissions of the three e-bus transit systems, all relevant components that produce GHG emissions are considered, as listed in Table 5, such as charging infrastructure construction, electricity transmission infrastructure (e.g., connection wires and cables), power electronic devices (e.g., inverters, transformers, and coils), and roadway retrofitting (e.g., pavement). The costs of these GHG emissions are provided in Appendix A. The GHG emission costs for different e-bus transit systems can be calculated via (10),

$$F_{GHG,facility} = \begin{cases} F_{GHG,end} + \sum_{i \in \mathcal{J}} x_i F_{GHG,opp}, & \text{for an SCS system,} \\ F_{GHG,bss}, & \text{for a BSS system,} \\ F_{GHG,end} + F_{GHG,chargingline}, & \text{for a DWCL system.} \end{cases} \tag{10}$$

where $F_{GHG,end}$, $F_{GHG,opp}$, $F_{GHG,bss}$, and $F_{GHG,chargingline}$ denote the GHG emission costs of the end-terminal charging station, opportunity charging station, battery swapping station, and dynamic charging lanes, respectively. Specifically, these GHG emission costs can be calculated based on the relevant components, as shown in (11) to (14). The detailed GHG emission factors and their parameter values are given in Appendix A.

$$F_{GHG,end} = a_{con} S_{end_{floor}} + a_{char} n_{end_{char}} + a_{wire} l_{end_{length}} + a_{trans} + a_{inv}, \tag{11}$$

$$F_{GHG,opp} = a_{con} S_{opp_{floor}} + a_{char} n_{opp_{char}} + a_{wire} l_{opp_{length}} + a_{trans} + a_{inv}, \tag{12}$$

$$F_{GHG,bss} = a_{con} S_{BSS_{floor}} + a_{char} n_{BSS_{char}} + a_{wire} l_{BSS_{length}} + a_{trans} + a_{inv}, \tag{13}$$

$$F_{GHG,chargingline} = \sum_{i \in \mathcal{J}} z_i (a_{inv} + a_{trans} + a_{coil}) + \sum_{i \in \mathcal{J}} d_i (a_{pav} + a_{wire} + a_{feeder}). \tag{14}$$

The life-cycle emissions of e-buses involve four stages: the well-to-tank (WTT) stage, tank-to-wheel (TTW) stage, glider stage, and powertrain stage (Messagie, 2017). Table 6 shows a detailed description of the life-cycle emissions of e-buses compared with those of conventional diesel vehicles. For e-buses, the TTW stage can be omitted due to the emission-free nature of recharging (Nordelöf et al., 2019). Moreover, the glider and powertrain stages can be combined into equipment life-cycle (ELC) emissions (Nordelöf et al., 2014).

Based on the above analysis, the life-cycle emission costs of e-buses consist of the WTT and ELC costs. The WTT cost is incurred during electricity delivery from the energy source to the bus energy storage system. The ELC emission cost consists of the glider stage (e.g., bus manufacturing, maintenance, and recycling processes) and powertrain stage (e.g., the production processes for the motor, batteries, and electronics); thus, this cost is dependent mainly on the number of buses in a fleet Q, the number of deployed batteries n_{BA}, and the battery capacity E. The life-cycle GHG emission cost ($F_{GHG,e-bus}$) of e-buses is therefore calculated as follows:

$$F_{GHG,e-bus} = a_{WTT} l_{year,j} + a_{ELC} Q, \tag{15}$$

where a_{WTT} denotes the global warming impact in the WTT stage, $l_{year,j}$ is the total travel distance of all buses in year j, and a_{ELC} denotes the global warming impact in the ELC stage. $l_{year,j}$ can be calculated as follows:

$$l_{year,j} = \sum_{i \in \mathcal{J}} l_i f T N_{day,j}, \tag{16}$$

where $N_{day,j}$ denotes the number of operating days in year j, $\sum_{i \in \mathcal{J}} l_i$ denotes the length of a service circuit, and f and T denote the operating frequency and hours, respectively.

3.2.4. Replacement cost

The technology replacement cost (F_{REP}) includes two components: the battery replacement cost F_{REP_BA} and the bus replacement cost F_{REP_BUS},

Table 5
GHG emission-related components for different types of charging infrastructures.

Charging infrastructure	GHG emission components						
Wireless charging lane	Pavement	–	Connection wire	Inverter	Transformer	Underground feeder	Coil transmitter
Swapping station	Construction	Chargers	Connection wire	Inverter	Transformer	–	–
End-terminal charging station	Construction	Chargers	Connection wire	Inverter	Transformer	–	–
Opportunity charging station	Construction	Chargers	Connection wire	Inverter	Transformer	–	–

Notes: The GHG emissions associated with charging infrastructure construction include the following components: (1) manufacturing of building materials, (2) transporting building materials, (3) transporting construction equipment, (4) consuming energy from construction equipment, (5) transporting workers, and (6) disposing of construction waste.

Table 6
Life cycle emissions of e-buses.

Stages	Diesel vehicle	Electric vehicle
WTT stage	The fuel supply chain	Electricity delivery from energy sources to bus energy storage systems
TTW stage	Energy conversion in the vehicle	Energy conversion and distribution inside a bus
Glider stage	Manufacturing, maintenance, and recycling of the vehicle	Bus manufacturing, maintenance, and recycling processes
Powertrain stage	Manufacturing the motor, battery, and electronics	Motor, battery, and electronics production

$$F_{REP} = F_{REP\_BUS} + F_{REP\_BA}. \tag{17}$$

For all e-buses, as shown in (18), we use the straight-line depreciation method to calculate the annual renewal costs. The replacement cost of all e-buses is calculated based on C_{BUS}, the bus salvage value C_{SV_BUS}, the fleet size Q, and the number of replacements over the lifespan $(\tau_L/\tau_{BUS} - 1)$. Here, we introduce the discount rate because the length of time spent buying equipment strongly affects the capital cost. Ideally, investors would obtain a larger profit if they could buy a piece of equipment later. d_{rate} denotes the annual discount rate. The bus replacement period always follows the e-bus replacement guidance of the e-bus manufacturing enterprise. If $MOD(j, \tau_{BUS}) = 0$, then $\omega_{j\_BUS} = 1$.

$$F_{REP\_BUS} = \sum_{j=1}^{\tau_L} (C_{BUS} - C_{SV\_BUS}) Q \omega_{j\_BUS} (1 + d_{rate})^{-j}. \tag{18}$$

For lithium-ion batteries, capacity fading occurs under both usage and storage conditions, which correspond to cycling and calendar aging, respectively. A battery needs to be replaced when its capacity reaches the predefined lower limit. Retired e-bus batteries can subsequently be used for stationary energy storage applications, such as apartment power storage and emergency lighting. A battery's EoL is reached when its SoH falls below the predefined lower limit, which is regarded as a decision variable; e.g., ω_j denotes whether EoL is reached at the end of year j to facilitate the optimization of battery replacement in this work.

The battery needs to be replaced when its capacity reaches EoL (70 %) (Zhang et al., 2021). Note that retired batteries can still be repurposed for secondary storage or undergo material recycling, retaining salvage value after replacement. At the end of year j, the battery reaches SoH_j, and its salvage value is $C_{SV\_BA} SoH_j E$. If the battery reaches EoL at the end of year j, $\omega_j = 1$. Then, as shown in (19), the battery replacement costs can be calculated according to the initial battery cost C_{BA}, the year corresponding to EoL (in which $\omega_j = 1$), the remaining salvage value at EoL, the battery capacity E, and the number of batteries n_{BA}.

$$F_{REP_{BA}} = \sum_{j=1}^{\tau_L} \left(C_{BA} - C_{SV_{BA}} SoH_j\right) E \omega_j n_{BA} (1 + d_{rate})^{-j}. \tag{19}$$

The SoH of a battery in year j can be calculated by (20) with $SoH_0 = 100\%$.

$$SoH_j = SoH_0 \omega_j + SoH_{j-1}\left(1 - \omega_j\right) - \frac{\xi_{day} N_{day} \mathrm{V}}{E} \geq \mathrm{EoL}, \tag{20}$$

where ξ_{day}, N_{day}, and V are the daily capacity fading rate, the number of operation days per year, and the battery voltage, respectively. The daily battery fading rate is calculated based on the battery degradation model developed and used in previous works (Lam and Bauer, 2013; Xu et al., 2021; Zhang et al., 2021). For charge process i, the capacity fading rate can be obtained through

$$\xi\left(T_i, SoC_{\mathrm{avg},i}, SoC_{\mathrm{dev},i}, \mathrm{Ah}_i\right) = \left(k_{s1} SoC_{\mathrm{dev},i} \cdot e^{\left(k_{s2} \cdot SoC_{\mathrm{avg},i}\right)} + k_{s3} e^{k_{s4} SoC_{\mathrm{dev},i}}\right) e^{\left(-\frac{E_d}{R}\left(\frac{1}{T_i} - \frac{1}{T_{\mathrm{ref}}}\right)\right)} \mathrm{Ah}_i, \tag{21}$$

where

$$SoC_{\mathrm{avg}} = \frac{1}{\Delta \mathrm{Ah}_m} \int_{\mathrm{Ah}_{m-1}}^{\mathrm{Ah}_m} SoC(\mathrm{Ah}) d\mathrm{Ah}, \tag{22}$$

$$SoC_{\mathrm{dev}} = \sqrt{\frac{3}{\Delta \mathrm{Ah}_m} \int_{\mathrm{Ah}_{m-1}}^{\mathrm{Ah}_m} \left(SoC(\mathrm{Ah}) - SoC_{\mathrm{avg}}\right)^2 d\mathrm{Ah}}, \tag{23}$$

k_{s1}, k_{s2}, k_{s3}, and k_{s4} are constant parameters, Ah_{m-1} is the initial amount of charge processed before SoC_{avg} determination, Ah_m is the final amount of charge in the predefined period, and $\Delta \mathrm{Ah}_m$ is $\mathrm{Ah}_m - \mathrm{Ah}_{m-1}$. In this study, SoC_{avg} and SoC_{dev} can be further simplified as functions of $SoC_{\max}$ and $SoC_{\min}$, i.e., $SoC_{\mathrm{avg}} = \frac{SoC_{\max} + SoC_{\min}}{2}$ and $SoC_{\mathrm{dev}} = \frac{SoC_{\max} - SoC_{\min}}{2}$.

The daily capacity fading rate ξ_{day} can be further calculated for different e-bus transit systems as follows:

$$\xi_{day} = \begin{cases} \dfrac{\xi_{SCS,cycle} fT}{Q}, & \text{for an SCS system,} \\ \xi_{BSS,day}, & \text{for a BSS system,} \\ \dfrac{\xi_{DWCL,cycle} fT}{Q}, & \text{for a DWCL system.} \end{cases} \tag{24}$$

where $\xi_{SCS,cycle}$ and $\xi_{DWCL,cycle}$ denote the battery degradation over each operating cycle of an SCS system and a DWCL system, respectively, and $\xi_{BSS,day}$ denotes the daily battery degradation in a BSS. These degradation rates are related to the working conditions and environmental temperature. Since it is difficult to obtain the temperature variation of a battery, we use a simplified degradation model with a uniform temperature T_i of 25℃.

Specifically, for the SCS system, the cycle degradation $\xi_{SCS,cycle}$, involving one end-terminal charging, $\sum_{i\in\mathscr{I}} x_i$ opportunity charging, and I discharging instances, is expressed as:

$$\xi_{SCS,cycle} = \xi\left(T_{end}, SoC_{\text{avg},end}, SoC_{\text{dev},end}, \text{Ah}_{end}\right) + \sum\nolimits_{i\in\mathscr{I}} \xi\left(T_{i,d}, SoC_{\text{avg},i,d}, SoC_{\text{dev},i,d}, \text{Ah}_{i,d}\right) + \sum\nolimits_{i\in\mathscr{I}} \xi\left(T_{i,c}, SoC_{\text{avg},i,c}, SoC_{\text{dev},i,c}, \text{Ah}_{i,c}\right) x_i, \tag{25}$$

where

$$\text{Ah}_{i,d} = \frac{E_d l_i}{V_d}, \tag{26}$$

$$\text{Ah}_{i,c} = \frac{P_{c,o} t_{c,o}}{V_{c,o}}, \tag{27}$$

$$\text{Ah}_{end} = \frac{E(SoC_{max} - SoC_I)}{V_{c,end}}, \tag{28}$$

E_{km} denotes the energy consumption per km, and l_i is the distance from stop $i-1$ to stop i ($i \in \mathscr{I}$). $\text{Ah}_{i,d}$ denotes the final amount of charge during the discharging period, $\text{Ah}_{i,c}$ is the final amount of charge during one opportunity charging, and Ah_{end} is the final amount of charge during the end-terminal charging period.

For the BSS system, each charging and discharging cycle includes one swapping charging process and I discharge processes; hence, the daily degradation is

$$\xi_{BSS,day} = \frac{2\sum_{k\in\mathscr{K}} \delta\xi\left(SoC_{\text{avg},sc}, SoC_{\text{dev},sc}\right) \text{Ah}_{sc,k} \text{y}_k Q}{n_{BA}}, \tag{29}$$

where the final amount of charge in circuit k is described by

$$\text{Ah}_{sc,k} = \frac{E}{\text{V}}\left(SoC_k^{out} - SoC_k^{in}\right). \tag{30}$$

For the DWCL system, the degradation during each charging and discharging cycle, with one end-terminal charging cycle, $\sum_{i\in\mathscr{I}} z_i$ instances of enroute wireless charging, and I instances of discharging, can be calculated by

$$\begin{aligned} \xi_{DWCL,cycle} = {} & \xi\left(T_{end}, SoC_{\text{avg},end}, SoC_{\text{dev},end}, \text{Ah}_{end}\right) + \sum\nolimits_{i\in\mathscr{I}} \xi\left(T_{i,d}, SoC_{\text{avg},i,d}, SoC_{\text{dev},i,d}, \text{Ah}_{i,d}\right)\left((1-z_i) + z_i(l_i - d_i)\right) \\ & + \sum\nolimits_{i\in\mathscr{I}} \xi\left(T_{i,cl}, SoC_{\text{avg},i,cl}, SoC_{\text{dev},i,cl}, \left(\text{Ah}_{i,cl} + \text{Ah}_{i,d}\right)\right) z_i d_i. \end{aligned} \tag{31}$$

Furthermore, the charge transferred during each charging/discharging process can be calculated by:

$$\text{Ah}_{end} = \frac{E(SoC_{max} - SoC_I)}{V_{c,end}}, \tag{32}$$

$$\text{Ah}_{i,d} = \frac{E_{km} d_i}{V_d}, \tag{33}$$

$$\text{Ah}_{i,cl} = \frac{E_{c,l} - E_d}{V_{c,l}} \sum\nolimits_{i\in\mathscr{I}} d_i, \tag{34}$$

where $\text{Ah}_{i,d}$ denotes the final amount of charge during each discharging period, $\text{Ah}_{i,cl}$ is the final amount of charge during the enroute wireless charging i, and Ah_{end} is the final amount of charge during the end-terminal charging period.

3.3. Problem formulation for SCS systems

An SCS system, as shown in Fig. 2, includes a fixed end-terminal charging station and several opportunity charging stations located at intermediate bus stations. According to the assumptions in Section 3.1, an e-bus is fully charged to SoC_{max} at the end-terminal station indexed as bus stop 0, i.e.,

$$SoC_0^{out} = SoC_{max}. \tag{35}$$

To guarantee this, the charging power and time conditions at the end terminal should be satisfied:

$$\frac{P_{c,end}t_{end}}{E} \geq SoC_{max} - SoC_I. \tag{36}$$

During bus service, the unit energy consumption per kilometer is E_d, and accordingly, the decrease in battery SoC per kilometer is E_d/E. For bus stop i, the arriving SoC (i.e., SoC_i^{in}) can be recursively expressed as follows:

$$SoC_i^{in} = SoC_{i-1}^{out} - \frac{E_d l_i}{E}, i > 0. \tag{37}$$

To avoid over-discharging the bus battery, set

$$SoC_i^{in} \geq SoC_{min}. \tag{38}$$

If bus stop i is selected as an opportunity charging station, the binary variable x_i is set to 1. E-buses can be charged while stopping at bus stop i if the charging infrastructure is available. After each instance of opportunity charging at power $P_{c,o}$ and for charging time t_{stop}, the battery SoC increases from SoC_i^{in} to SoC_i^{out}, as shown below:

$$SoC_i^{out} = SoC_i^{in} + \frac{P_{c,o}t_{stop}x_i}{E}. \tag{39}$$

Moreover, to ensure sufficient buses for maintaining service frequency f, the following constraint is set: the total operating time of a bus includes the enroute travel time $\sum_i l_i/v$, the boarding and alighting time at bus stops It_{stop}, and the end-terminal charging time t_{end}.

$$Q \geq \left(\frac{\sum_i l_i}{v} + It_{stop} + t_{end}\right) f. \tag{40}$$

In the above formulation, the relevant variables are constrained as follows:

$$x_i \in \{0, 1\}, \tag{41}$$

$$\omega_j \in \{0, 1\}, \tag{42}$$

$$E \in \mathbb{N}^+, \tag{43}$$

$$Q \in \mathbb{N}^+. \tag{44}$$

For the SCS system model, the LCC F_{LCC}, as stated in (45), which consists of the capital cost F_{CAP}, operating cost F_{OP}, GHG emission cost F_{GG}, and technology replacement cost F_{REP} defined in Section 3.1., can be optimized by

$$minF_{LCC} = F_{CAP} + F_{OP} + F_{GG} + F_{REP}, \tag{45}$$

s.t. (2)-(44).

3.4. Problem formulation for BSS systems

For a BSS system, $k \in \mathscr{K} := \{1, 2, \cdots, K\}$ is the circuit index of an e-bus. The total number of circuits K during each day can be calculated from the frequency f, the number of daily operating hours T, and the fleet size Q and rounded up to the nearest integer as follows:

$$K = \left\lceil \frac{fT}{Q} \right\rceil. \tag{46}$$

A binary decision variable y_k is set to indicate whether the battery is swapped out at circuit $k \in \mathscr{K}$. Since the operating distance each day is constant, a new decision variable n_k is introduced to denote the number of circuits that the e-bus serves before swapping. Then, y_k can be obtained by

$$y_k = \begin{cases} 1, & \text{if } mod(i, n_k) = 0 \text{ or } k = K, \\ 0, & \text{otherwise.} \end{cases} \tag{47}$$

According to the assumptions in Section 3.1, the bus is already fully charged to SoC_{max} before the first departure in the morning, i.e.,

$$SoC_0^{out} = SoC_{max}. \tag{48}$$

For each circuit, the operating distance is $\sum_{i\in\mathscr{J}} l_i$, and the power consumption is $E_d\sum_{i\in\mathscr{J}} l_i$. Then, we can obtain the SoC decrease, i.e., $\sum_{i\in\mathscr{J}} l_i E_d/E$. When an e-bus finishes circuit k and returns to the BSS, its SoC is denoted by SoC_k^{in}. Next, when the e-bus leaves the BSS for circuit $k+1$, its SoC is denoted by SoC_k^{out}. This relationship can be expressed as follows:

$$SoC_k^{in} = SoC_{k-1}^{out} - \frac{E_d}{E}\sum\nolimits_{i\in\mathscr{J}} l_i. \tag{49}$$

Depending on the battery swapping status in circuit k, i.e., y_k, the departing SoC of circuit k is

$$SoC_k^{out} = SoC_{max} y_k + SoC_k^{in}(1 - y_k). \tag{50}$$

To ensure that the battery SoC never falls below its lower bound SoC_{min}, the following constraint is set

$$\mathrm{SoC}_k^{in} \geq SoC_{min}. \tag{51}$$

If the current battery SoC is above SoC_{min}, the following SoC_{safe} is introduced to guarantee that the e-bus is able to return to its departure station in the current circuit. All the buses are fully charged at the end of the day, e.g., $y_K = 1$.

$$My_k \geq SoC_{safe} - SoC_k, \tag{52}$$

$$SoC_{safe} = SoC_{min} + \frac{E_d\sum_{i\in\mathscr{J}} l_i}{E}. \tag{53}$$

Moreover, to ensure that sufficient e-buses are operating in the bus system, we set

$$Q \geq \left(\frac{\sum_i l_i}{v} + It_{stop} + \frac{t_{swap}}{n_k}\right) f. \tag{54}$$

At the swapping station, the exhausted batteries are replaced with fully charged batteries and then recharged. The recharging process lasts less than $t_{c,s}$. To maintain consistent service, redundant batteries are needed. Thus, the number of batteries must satisfy

$$n_{BA} - Q - \frac{ft_{c,s}\sum_{k\in\mathscr{K}\setminus\{K\}} y_k}{K} \geq 0. \tag{55}$$

The formulated optimization problem for BSSs involves four decision variables: the battery swapping status for circuit k, i.e., y_k, the initial battery energy capacity E, the bus fleet size Q, and the battery number n_{BA}, which are constrained by

$$y_k \in \{0, 1\}, \tag{56}$$

$$n_k \in \mathbb{N}^+, \tag{57}$$

$$n_{BA} \in \mathbb{N}^+. \tag{58}$$

For the BSS system model, the objective function of the optimization problem is consistent with that of the SCS system, as given in (45); however, the following constraints are considered: (2)-(34) and (46)-(58).

3.5. Problem formulation for DWCL systems

As mentioned above, a DWCL system is composed of a fixed end-terminal charging station and a few dynamic charging lanes between bus stations. The SoC_0^{out}, charging power, and time constraints for the DWCL system at the end-terminal station are similar to those of the SCS system, as described in (35) and (36).

When an e-bus travels from bus stop $i-1$ to bus stop i, the DWCL charging energy per kilometer is $E_{c,l}$, and the battery discharging energy per kilometer is E_d. Then, the arriving SoC can be recursively calculated by

$$SoC_{i+1} = SoC_i + \frac{E_{c,l} d_i z_i - E_d(l_i - d_i)}{E}. \tag{59}$$

Again, the battery SoC has a lower bound to avoid overdischarge, i.e.,

$$SoC_i \geq SoC_{min}. \tag{60}$$

Moreover, the constraint on the number of buses for the DWCL system is the same as that for the SCS system, as shown in (40).

For the DWCL system, four decision variables are involved in the problem formulation: Here, the binary variable z_i indicates whether the link from stop $i-1$ to stop i is a charging link, the length of the charging lane d_i, the initial battery size E, and the bus fleet size Q. The following constraints for decision variables are established:

$$z_i \in \{0, 1\}, \tag{61}$$

Table 7
Parameter definitions and values.

Notation	Definition	Value	Unit	Data source
E	Battery capacity	60–400	kWh	(Xylia et al., 2019)
f	Service frequency	12	veh/h	ITDP website
T	Operating hours, h	18	h	ITDP website
$sum(l_i)$	Total circuit length	45	km	ITDP website
°C	Average operational temperature	25	℃	(Zhang et al., 2021)
$N_{day,j}$	Average days of operation in year j	365	–	ITDP website
t_{stop}	Average stop time for alighting and boarding	0.02	h	(Pei et al., 2021)
t_{end}	Maximum charging time for an end-terminal station	1	h	(Andersson, 2017)
$t_{c,s}$	Maximum charging time for an exhausted battery at a swapping station	3.5	h	(Zhang et al., 2021)
t_{swap}	Time to swap out a battery	0.1	h	(Zhong and Pei, 2020)
v	Average bus speed	18	km/h	ITDP website
d_{rate}	Discount rate	0.05	–	(Zhang et al., 2021)
τ_L	Estimated life cycle period	50	years	(Chatzikomis et al., 2014)
τ_{bus}	E-bus replacement period	12	years	(Zhang et al., 2021)
C_β	Monetary value of emissions	0.15	$/kg	(Liang et al., 2019)
a_{WTT}	100-year global warming impact based on WTT	0.02	kg/km	(Nordelöf et al., 2014)
a_{ELC}	100-year global warming impact based on ELC	Glider:0.035 Powertrain:170	kg/km kg/kWh	(Nordelöf et al., 2014)
SoC	EV battery SoC, with the range $[SoC_{min}, SoC_{max}]$	[20 %,100 %]	–	(Zhang et al., 2021)
$P_{c,o}$	Charging power for an opportunity charge station	120	kW	(Volvo Bus Corporation, 2019)
$P_{c,end}$	Charging power for an end-terminal charge station	120	kW	(Chen et al., 2018)
$P_{c,s}$	Charging power for a swapping station	120	kW	(Chen et al., 2018)
$P_{c,l}$	Charging power for a wireless charging lane	80	kW	(Chen et al., 2018)
$E_{c,l}$	Energy charged per km along a dynamic charging lane (kWh/km)	3	kWh/km	(Ahmad et al., 2017)
E_d	Battery energy consumption per km (kWh/km)	1.35	kWh/km	(Zhang et al., 2021)
EoL	Battery end of life	0.7	–	(Zhang et al., 2021)
$V_{c,o}$	Average charging voltage for an opportunity charging station	380	V	(Andersson, 2017)
$V_{c,end}$	Average charging voltage an end-terminal charging station	380	V	(Andersson, 2017)
$V_{c,s}$	Average charging voltage for a swapping station	380	V	(Andersson, 2017)
$V_{c,l}$	Average charging voltage for a dynamic charging lane	380	V	(Gong et al., 2018)
V_d	Average discharging voltage	316	V	(Zhang et al., 2021)
C_{BA}	Unit battery purchase cost per kWh	200	$/kWh	(Chen et al., 2018)
C_{BUS}	Initial bus purchase cost	315,320	$	(Chen et al., 2018; Guangzhou Bus Group, 2022)
$C_{m,bus}$	Unit bus maintenance cost per year	5700	$	(Hassold and Ceder, 2014)
$C_{m,ba}$	Unit battery maintenance cost per year	5700	$	(Hassold and Ceder, 2014)
$C_{m,infra..end}$	Charging infrastructure maintenance cost for an end-terminal charging station per year	10,000	$	(Hassold and Ceder, 2014)
$C_{m,infra..opp}$	Charging infrastructure maintenance cost for an opportunity charging station per year	4000	$	(Hassold and Ceder, 2014)
$C_{m,infra..BSS}$	Charging infrastructure maintenance cost for a swapping station per year	10,000	$	(Hassold and Ceder, 2014)
$C_{m,infra.length}$	Charging infrastructure maintenance cost for a wireless charging lane per year	4000	$	(Hassold and Ceder, 2014)
C_{SV_BUS}	Unit salvage value of a bus	0	$/veh	(Zhang et al., 2021)
C_{SV_BA}	Unit salvage value of bus batteries per kWh	48	$/kWh	(Sierzchula et al., 2014)
C_{end}	Construction cost for an end-terminal charging station	300,000	$	(Sierzchula et al., 2014)
$C_{c,o}$	Construction cost for an opportunity charging station	50,000	$	(Sierzchula et al., 2014)
$C_{c,s}$	Construction cost for a BSS	562, 400	$	(Chen et al., 2018)
$C_{c,t}$	Construction cost for the inverter in a DWCL	20,000	$	(Chen et al., 2018)
$C_{c,l}$	Unit construction cost for a DWCL per km	201,125	$/km	(Chen et al., 2018)
$C_{p,end}$	Unit energy fee for an end-terminal charging station	0.11	$/kWh	(Zhang et al., 2021)
$C_{p,o}$	Unit energy fee for an opportunity charging station	0.11	$/kWh	(Zhang et al., 2021)
$C_{p,s}$	Unit energy fee for a BSS	0.11	$/kWh	(Zhang et al., 2021)
$C_{p,l}$	Unit energy fee for a DWCL	0.11	$/kWh	(Zhang et al., 2021)
α_{end}	Charging efficiency for an end-terminal charging	0.9	–	(Bi et al., 2017; Chen et al., 2018)
$\alpha_{c,o}$	Charging efficiency for an opportunity charging	0.9	–	(Volvo Bus Corporation, 2019)
$\alpha_{c,s}$	Charging efficiency for swapping battery charging	0.9	–	(Chen et al., 2018)
$\alpha_{c,l}$	Charging efficiency for a DWCL	0.8	–	(Chen et al., 2018)
k_{s1}	Coefficient in the battery capacity fading model	−4.09E-4	–	(Lam and Bauer, 2013)
k_{s2}	Coefficient in the battery capacity fading model	−2.167	–	(Lam and Bauer, 2013)
k_{s3}	Coefficient in the battery capacity fading model	1.418E-5	–	(Lam and Bauer, 2013)
k_{s4}	Coefficient in the battery capacity fading model	6.13	–	(Lam and Bauer, 2013)

Note: ITDP indicates the Institute of Transportation & Development Policy (Website: https://www.itdp.org/).

$$d_i \in \mathbb{N}^+. \tag{62}$$

For the DWCL system, the formulation of the optimization problem is consistent with other systems, i.e., (45), s.t. (2)-(36), (40) and (59)-(62).

4. Parameterization and implementation

The parameter values used to solve the optimization problems formulated in Section 3 are listed in Table 7. Some parameter values vary due to temporal and geographical factors. All e-bus charging infrastructures are assumed to involve fixed construction areas and costs. According to previous studies (Chen et al., 2018; Nie and Ghamami, 2013), the construction area for one end-terminal charging station involves a fixed building as well as several buses, and the construction of an end-terminal charging station is assumed to cost $300,000. Moreover, the total construction cost for one swapping station is approximately $562,400 (Chen et al., 2018; Nie and Ghamami, 2013). The construction cost of one charging lane segment is $201,125 per km, and the unit inverter cost is $20,000 (Liu et al., 2019). The bus purchase price without batteries is $315,320. The battery price for an e-bus can range from $137/kWh to $700/kWh (BloombergNEF, 2020; Pathak et al., 2021; Statusrapport, 2020; Zeng et al., 2022). We use $300/kWh as the default battery price and present a supplemental sensitivity analysis for prices ranging from $100/kWh to $700/kWh in Section 5.2. The parameters in the battery degradation model, e.g., k_{s1}, k_{s2}, k_{s3} and k_{s4}, are obtained from Lam and Bauer (2013). The battery needs to be replaced when its capacity reaches EoL (70 %) (Zhang et al., 2021). However, replacement batteries can still be used for other purposes. The unit battery price is expected to decrease as associated battery technology advances, which will significantly affect the cost competitiveness of e-bus transit systems.

According to Bi et al. (2015), the charging efficiency of plug-in chargers deployed at charging stations and swapping stations is assumed to be 90 %. The charging efficiency of a DWCL is assumed to be 85 %, and additional energy transfer loss occurs during long-distance wireless charging. The average electricity fee per kWh slightly varies for different charging facilities and in different cities.

Note that the parameter values are taken from different mainstream literature articles, and there may be some mismatches. However, the model and framework developed in this paper are generic and can be used in comprehensive competitive analyses of multiple charging solutions based on actual city-specific parameter values.

Due to the nonlinear components in the battery degradation model and the related battery replacement mechanisms, the problems formulated in Section 3 include nonlinear programming. To solve these problems, we use a branch-and-bound-type solver, i.e., BNB20

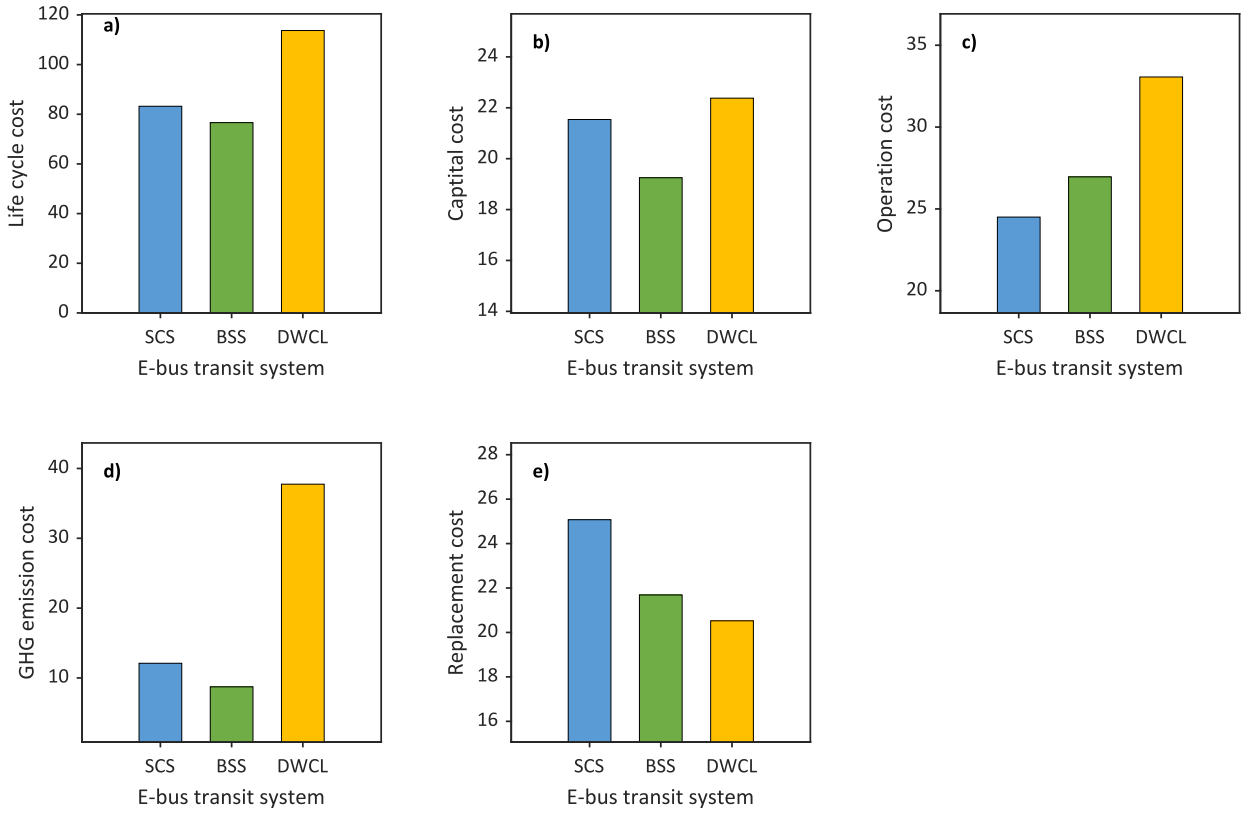

Fig. 3. Comparisons of the detailed costs of three e-bus transit systems based on bus line B1 in Guangzhou, China. (a) Life cycle cost (million $); (b) capital cost (million $); (c) operating cost (million $); (d) GHG emission cost (million $); (e) replacement cost (million $).

in MATLAB, designed for nonlinear programming. Solutions and discussions are based on the default values, except for the sensitivity analysis.

5. Results and discussion

5.1. Case study of Guangzhou B1 bus route

To evaluate the utility of the three e-bus transit systems and the cost competitiveness of charging strategies, bus line B1 in Guangzhou, China, is used as a representative scenario. The length of bus line B1 is 45 km, and 52 bus stops are included in the total trip circuit. E-buses operate on the B1 line from 06:00 to 24:00 every day, corresponding to 18 operating hours (T). The peak-hour service frequency is 12 circuits/hour, and the average speed of travel in the bus rapid transit (BRT) corridor is 18 km/h. E-buses on the B1 line have been operating on a BRT corridor since June 2014. In August 2020, all the vehicles used for the B1 line were pure electric buses. To meet the increasing demand for e-bus charging, a charging parking lot is constructed at the terminal.

We investigate the cost competitiveness of three types of e-bus transit systems based on their corresponding optimal solutions. The detailed cost components of the different systems are compared in Fig. 3, and each LCC is presented for the entire system. The bar charts in Fig. 4 present a comparison of the results for the SCS, BSS, and DWCL systems in terms of the optimal bus fleet size, required battery number, battery energy capacity, and battery replacement period.

As shown in Fig. 3(a), the LCC of the BSS system is lower than those of the SCS and DWCL systems. Specifically, the LCC of the BSS system is 76.6 million dollars, which is 8.6 % and 48.4 % lower than the costs of the SCS and DWCL systems, respectively. Fig. 3(b)–(e) also compare the capital, operating, emission, and replacement costs, respectively. The sizes of the bus fleets in all three systems are shown in Fig. 4(a), and the fleet size is mainly related to the charging time; notably, a longer charging time requires a larger fleet size to cover the service frequency if all other parameters remain unchanged. The fleet size of the BSS system is smaller than that of the SCS and DWCL systems since the battery swapping time is significantly shorter than the terminal charging time in other alternative systems. In addition, as shown in Fig. 4(c), the battery energy capacity of the BSS system is the largest among the three systems since batteries are charged only at the fixed swapping station after several rounds of service, while the SCS and DWCL systems allow charging between bus stops. Such enroute services can effectively reduce the required battery capacity. In particular, in the DWCL system, the wireless charging lane setup greatly reduces the battery size to the minimum.

As shown in Fig. 3(b), for the Guangzhou B1 bus line scenario, the capital costs of the SCS, BSS, and DWCL systems, including the

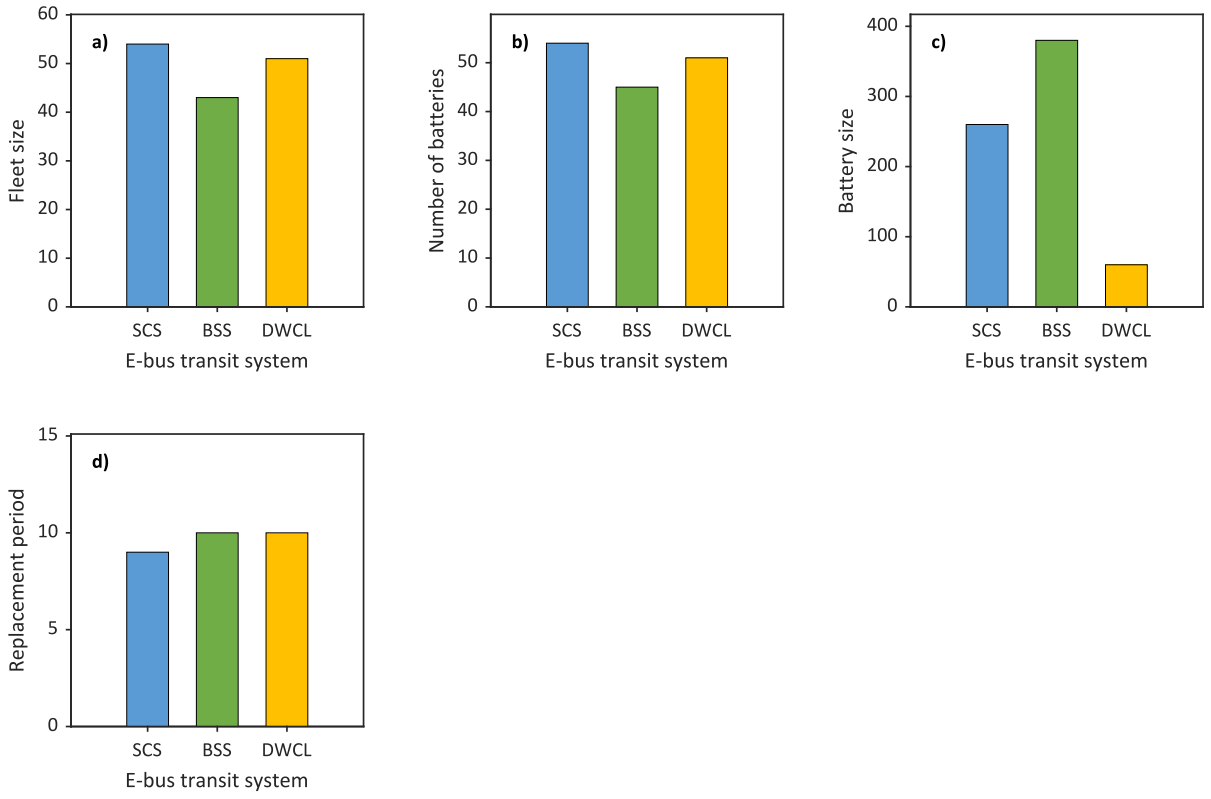

Fig. 4. Comparisons of three e-bus transit systems based on bus line B1 in Guangzhou, China. (a) e-bus fleet size (vehicles); (b) number of required batteries; (c) battery size or battery energy capacity (kWh); (d) battery replacement period (years).

infrastructure construction cost and the purchase costs of e-buses and batteries, are similar at 21.5 million dollars, 19.3 million dollars, and 22.4 million dollars, respectively. The capital cost of the DWCL system is approximately 16 % greater than that of the BSS system. Specifically, the infrastructure construction and purchase costs are detailed in Fig. 5(a)-(c). The results show that the DWCL system has the highest infrastructure construction cost (5.3 million dollars), as shown in Fig. 5(a). This is due to the very high construction cost of wireless charging lanes. However, as shown in Fig. 5(b), the battery purchase cost for the DWCL system (0.97 million dollars) is much lower than that for the SCS and BSS systems at approximately one-fifth of that of the BSS system and a quarter of that of the SCS system. The high battery cost of the BSS and low battery cost of the DWCL result from the corresponding high battery capacities, as shown in Fig. 4(c). In addition, the bus purchase cost is the highest of the capital costs for the three e-bus transit systems, as demonstrated in Fig. 5(c). The bus purchase cost for the BSS is 13.56 million dollars, lower than those for the SCS and DWCL systems. According to Chen et al. (2018) and the bid announcement for a pure electric bus procurement project in Guangzhou (Guangzhou Bus Group, 2022), the e-bus purchase price ranges from $122,202 to $315,320, which strongly influences the capital cost. Furthermore, a sensitivity analysis of these key parameter values is conducted in Section 5.2.

Moreover, the replacement costs are compared in Fig. 3(e), and the DWCL system has the lowest replacement cost. The total replacement cost includes two components: the battery replacement cost and the bus replacement cost. The low battery capacity in the DWCL system, as shown in Fig. 4(c), corresponds to low battery replacement costs. Moreover, the SCS and DWCL systems require more electric bus vehicles than does the BSS system, as shown in Fig. 4(a), resulting in higher bus replacement costs. Based on the combined replacement costs of batteries and buses, the highest replacement cost is observed for the SCS system, and the lowest is associated with the DWCL system, as shown in Fig. 3(e).

The operating costs of the three systems decrease from the BSS system to the DWCL system, as shown in Fig. 3(c). The total operating cost during the life cycle consists of the energy consumption cost ($F_{energy,j}$) and the maintenance cost ($F_{maint.,j}$), as shown in Fig. 6. Because the power transfer efficiency of the wireless charging lane (a component of the DWCL) is lower than that of the BSS and SCS, the $F_{energy,j}$ of the DWCL is the highest among the three systems according to Equation (7), as shown in Fig. 6(b). For the three systems, as expressed in (8), the maintenance costs of each bus and certain infrastructure are constant, so the maintenance cost depends on the number of buses (i.e., Q or n_{BA}) in the fleet and the e-bus transit system applied. The optimization results for the B1 bus line show that the BSS system has the lowest maintenance cost, mainly due to having the smallest number of batteries and smallest fleet size, as observed in Fig. 4(b).

An environmental analysis of the three e-bus transit systems in terms of the emission cost is shown in Fig. 7. The emission cost consists of two parts: bus emissions and facility emissions. The emission cost of the DWCL system is the highest at 37.61 million dollars, approximately three times greater than the average of the other two systems. The DWCL system has the highest cost for charging infrastructure, as shown in Fig. 5(a), i.e., for underground facilities and pavements, which also leads to high levels of GHG emissions. On the other hand, the emission costs are much lower for the SCS and BSS systems due to the differences between bus system requirements and charging infrastructure components.

5.2. Sensitivity analysis results

System parameter values can strongly affect the cost competitiveness of the investigated e-bus transit systems. Hence, in this section, we perform sensitivity analyses of the optimal LCC performance of each system for various parameter values and combinations of parameters, such as the e-bus transit system parameters (e.g., the number of bus stops, length of the bus line, service frequency of the bus line, and bus travel speed), the current battery characteristics (e.g., the battery degradation rate and battery price), and other vital parameter values (e.g., the life cycle period, the monetary rate for GHG emissions, and the purchase price of each bus).

5.2.1. Sensitivity analysis to various parameter values

Fig. 8 summarizes the sensitivity analysis results, in which the blue, green, and yellow curves denote the optimal LCCs of the SCS,

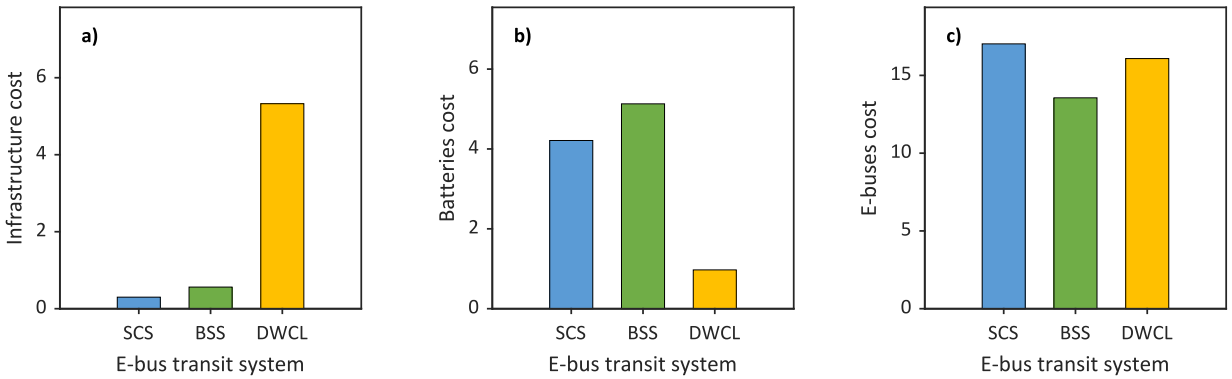

Fig. 5. Comparisons of the capital cost components of three e-bus transit systems based on bus line B1 in Guangzhou, China. (a) Infrastructure cost; (b) initial battery purchase cost (million dollars); (c) initial e-bus purchase cost (million dollars).

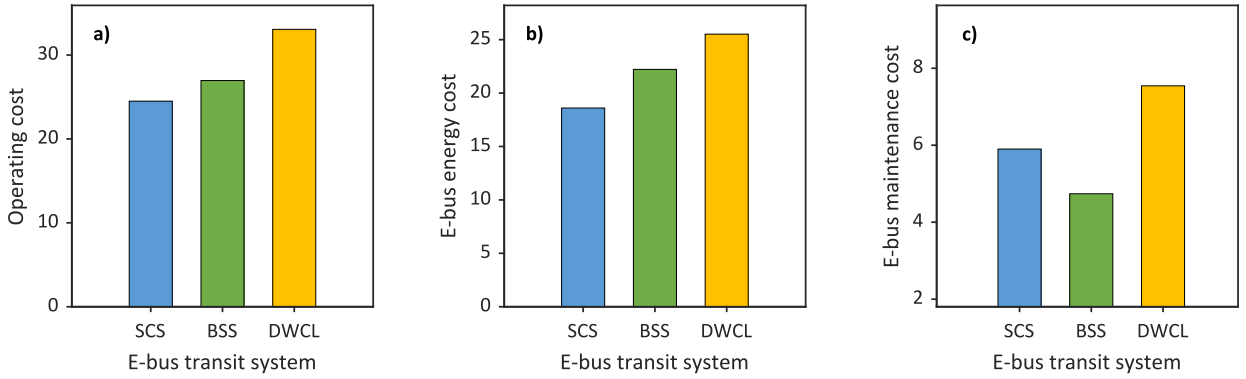

Fig. 6. Comparisons of the operating cost components of three e-bus transit systems based on bus line B1 in Guangzhou, China. (a) Operating cost (million $); (b) e-bus energy cost (million $); (c) e-bus maintenance cost (million $).

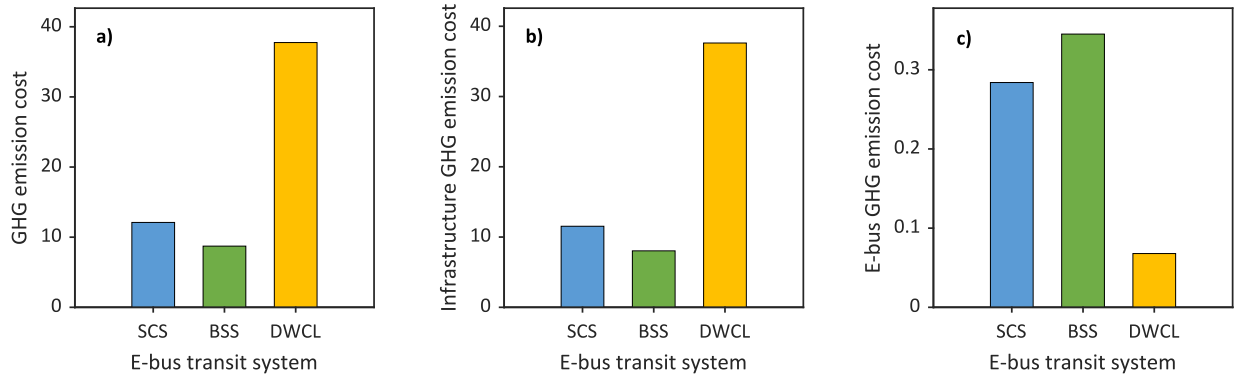

Fig. 7. Comparisons of GHG emission costs of three e-bus transit systems based on bus line B1 in Guangzhou, China. (a) GHG emission cost; (b) Infrastructure GHG emission cost; (c) E-bus GHG emission cost. Unit: million USD.

BSS, and DWCL systems, respectively. These optimal LCCs for different systems change significantly with varying parameter values.

For all charging systems, the LCCs increase as each parameter increases except for the average speed of travel, which is negatively correlated with the LCC. Generally, the BSS system has a lower LCC than the other systems. Additionally, it outperforms the other systems for most parameter values, mainly due to the low capital costs and bus replacement costs associated with the smaller fleet size of the BSS system. For example, the DWCL system features higher construction and GHG emission costs, and the SCS has higher capital and replacement costs than does the BSS because it involves more e-buses.

Specifically, as shown in Fig. 8(a), the LCC increased for all systems as the number of bus stops increased, but there was no significant difference in the rate of the increase. The construction and GHG emission costs for DWCLs are greater than those of other systems. Fig. 8(b) shows that the LCC of the BSS system is the lowest when the bus line length is less than 110 km, and the optimal solution is achieved with the SCS system for bus lines longer than 110 km. The buses in the BSS are only powered at the end of the circuit when the battery is swapped; thus, the route length influences the magnitude of the SoC, further influencing the battery degradation process and replacement cost. When the length is longer than 110 km, the replacement cycle of the battery in the BSS system is two years, and the replacement cost is approximately half of the total LCC. Fig. 8(c) shows the LCCs of the different systems with increasing service frequency f. Notably, the BSS system has a lower cost than the other systems. Next, Fig. 8(d) and (e) focus on the battery price and degradation, which are expected to gradually decrease with advanced battery technology. With decreases in the battery price and degradation rate, the LCCs for the SCS and BSS systems drop more rapidly than that for the DWCL system since a much smaller battery size is required in the DWCL system. Fig. 8(f) shows that the LCCs of the SCS and BSS are lower and less sensitive to the LCC analysis period than is the LCC of the DWCL system. Fig. 8(g) shows that the LCCs decrease as the average bus travel speed increases. When the bus travel speed increases, smaller fleet sizes can cover the required service frequency, which is consistent for all systems. For the GHG emission cost, as shown in Fig. 8(h), the DWCL system is more sensitive to the unit cost of emission since it the initial GHG cost is high in the facility construction process. Finally, Fig. 8(i) shows that the LCC sensitivity of the BSS system to the bus purchase price is slightly lower than that for the SCS and DWCL systems because fewer buses are involved.

The LCC for each system fluctuates with different parameter values, e.g., in Fig. 8(b), (e), (f), and (g), and some interesting analysis results can be further revealed. First, for the given parameter values, although the BSS system is more economically competitive in general, the SCS system may exhibit better competitiveness for long bus lines. Moreover, the DWCL system is currently not

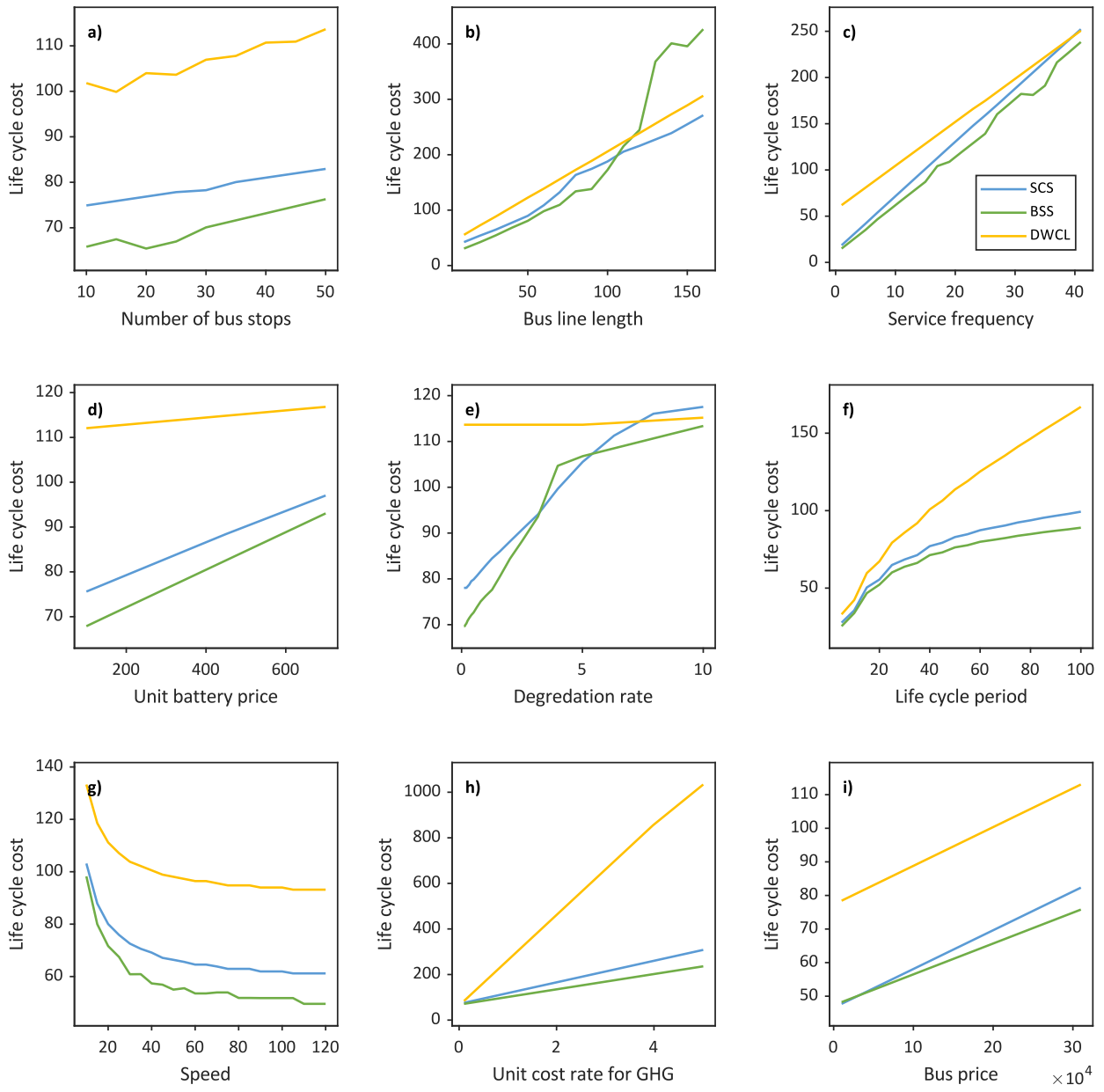

Fig. 8. LCC sensitivity analysis. (a) Number of bus stops; (b) bus line length (km); (c) service frequency *f* (veh/h); (d) unit battery price ($/kWh); (e) degradation rate (%); (d) life cycle period (years); (g) average bus travel speed (km/h); (h) monetary value for GHG ($/kg); and (i) bus price ($).

recommended when considering GHGs since the emission cost of the DWCL system is much greater than that of the SCS and BSS systems. For the DWCL system, however, the high emission cost and LCC for each bus line can be mitigated when multiple bus lines share the same charging infrastructure, which will be further discussed later in the section.

As one important component of the LCC, the replacement cost for each type of e-bus transit system, as defined in Equations (17)-(19), increases with increasing parameter values, as shown in Fig. 9. In Fig. 9(a), various unit battery prices are considered, and the replacement cost for the DWCL system is the lowest when the unit battery price exceeds $250/kWh. The BSS and SCS systems are more sensitive to the unit battery price than is the DWCL system because the battery capacities of the BSS and SCS systems are greater than that of the DWCL system over a similar replacement period. Moreover, as the service frequency or bus line length increases, as shown in Fig. 9(b) and Fig. 9(c), the total annual travel distance increases, leading to a shorter replacement period and thus increasing replacement costs. As shown in Fig. 9(c), the replacement cost for the BSS system increases dramatically for bus lines longer than 70 km. Because the BSS system includes only charging at terminals, batteries experience a deeper discharge as the length of the bus line increases, expediting battery degradation and shortening the battery replacement period. Consequently, a steep escalation in the replacement cost of the BSS system is observed.

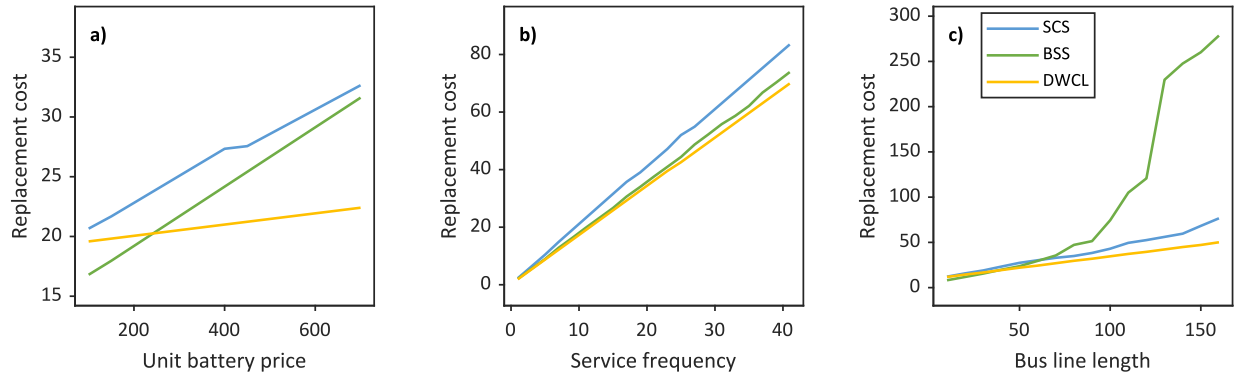

Fig. 9. Sensitivity of the replacement cost to the (a) unit battery price ($/kWh), (b) service frequency (veh/h), and (c) bus line length (km).

Another component of the LCC is the GHG emission cost, as shown in Fig. 10, which increases linearly with the monetary rate and the life cycle period but remains almost constant at varying travel speeds, unit battery prices, and service frequencies. In addition, as shown in Fig. 10(d) and (f), the GHG emission cost of the SCS system increases at certain unit battery costs or service frequencies. The major reason is that the required number of opportunity charging stations increases when optimizing the SCS system design at such unit battery costs or service frequencies. As illustrated in Fig. 7, the impact of charging infrastructure construction, e.g., the construction of opportunity charging stations, on the emission cost is dominant. Thus, at the aforementioned unit battery costs and service frequencies, the increasing need for opportunity charging stations leads to pronounced fluctuations in GHG emission costs. Due to the sizeable GHG emission costs, the DWCL system appears to be the least competitive from an environmental perspective. In particular, as shown in Fig. 10(c), the GHG emission cost of the SCS system notably increases within the 50–100 km range. With the extension of bus lines, additional opportunity charging infrastructures are progressively integrated into the SCS system until all stations are equipped. Consequently, the increased quantity of opportunity charging infrastructures significantly increases infrastructure GHG emission costs.

In addition, battery capacity is a significant component of costs throughout the entire lifecycle and is influenced by various factors.

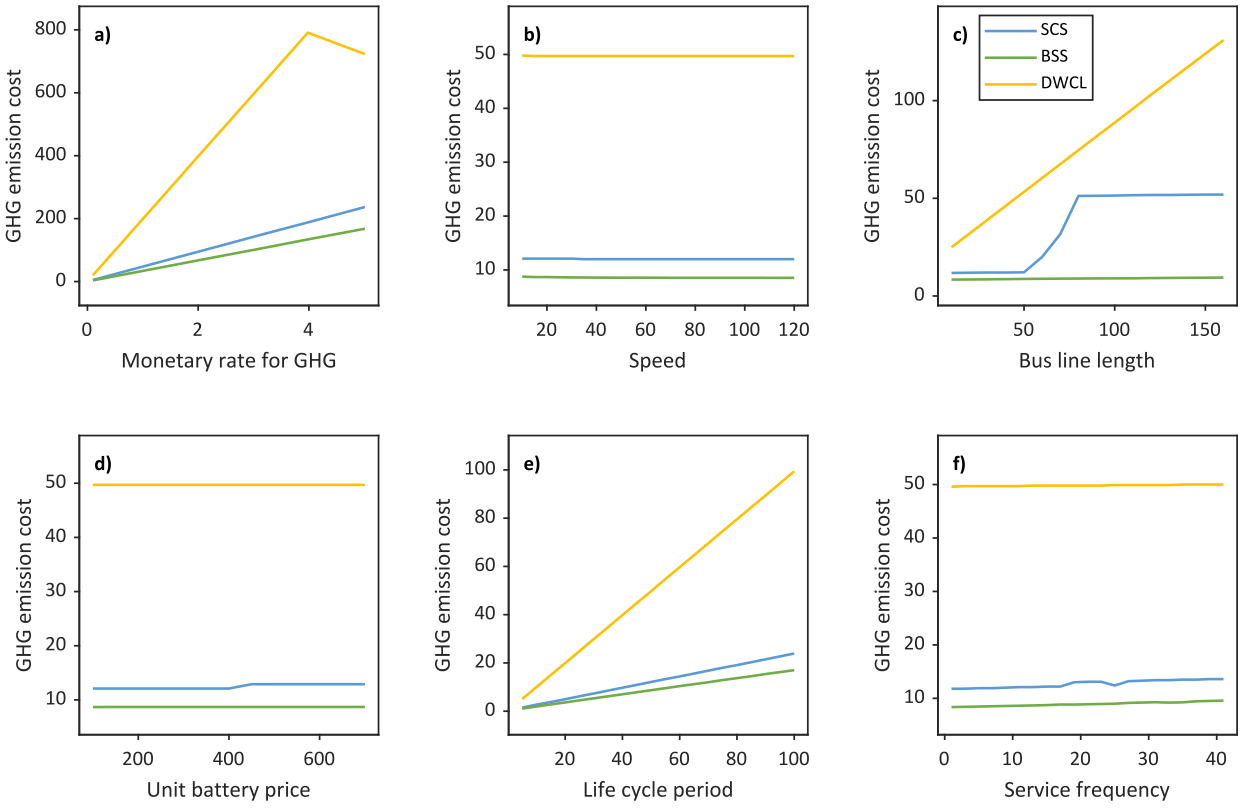

Fig. 10. Sensitivity of GHG emission cost to (a) the monetary rate for GHG emissions ($/kg); (b) travel speed (km/h); (c) bus line length (km); (d) unit battery price ($/kWh); (e) life cycle period (year); and (f) service frequency (veh/h).

Consequently, the impact of various parameter values on the required battery capacity for this case study is analyzed in Fig. 11. As shown in Fig. 11(a), given that the battery capacity is limited to 60 to 400 kWh, the DWCL and BSS systems reach the lower and upper capacity limits, respectively. The relatively minor variation in the battery capacity of the SCS system is due to the requirement that the battery capacity be sufficient to meet the service frequency for the bus line. The BSS and SCS slopes are similar for short bus line lengths. However, for moderate-range bus line lengths, the significant difference between the BSS and SCS is associated with the ability of the SCS system to reduce battery capacity based on the increased construction of opportunity charging infrastructure, as presented in Fig. 11(b). Furthermore, when the battery degradation rate decreases, as shown in Fig. 11(c), both the SCS and BSS systems generally require smaller battery capacities. As shown in Fig. 11(d–f), the battery capacities of the SCS and BSS systems exhibit uncertain fluctuations as the speed, life cycle period and service frequency change since the optimal choice of battery capacity is influenced by multiple factors.

5.2.2. *Sharing charging infrastructure among multiple bus lines*

Practical e-bus transit systems can involve multiple bus lines. Fig. 12 shows the sensitivity analysis results of the LCC and the associated component costs when the charging infrastructure is shared among multiple lines. As shown in Fig. 12(a), when the number of bus lines increases, the LCC of each bus line decreases for all three types of systems. The LCC of the DWCL system decreases most sharply because the initial capital cost (including the high construction cost) (Fig. 12 (b)) and GHG emission cost (Fig. 12(c)) of the system are shared by all involved lines. On the other hand, the operating cost in Fig. 12(d), which consists of the power consumption and maintenance costs, and the replacement cost in Fig. 12(e) do not vary much due to the use of additional lines.

5.2.3. *Sharing the charging infrastructure with private electric cars*

To meet the charging demands of private electric vehicles and improve the utilization rate of bus charging stations, 19 bus charging stations, including 234 charging systems in Guangzhou, China, are fully open to private electric cars under the premise of ensuring bus charging (Wang, 2021). Therefore, we analyzed the cost performance with varying e-bus percentages in Fig. 13. For SCS and DWCL systems, the construction, maintenance and emission costs of opportunity charging stations and wireless charging lanes can be shared with private cars. However, the battery replacement and swapping services are shared in a BSS system. Thus, the analysis is focused on the SCS and DWCL systems.

As shown in Fig. 13(a), the LCCs of the DWCL and SCS systems increase as the percentage of e-buses increases. The LCC of the DWCL system is most sensitive to the e-bus percentage. When the bus percentage is less than 30 %, the DWCL system is more competitive than

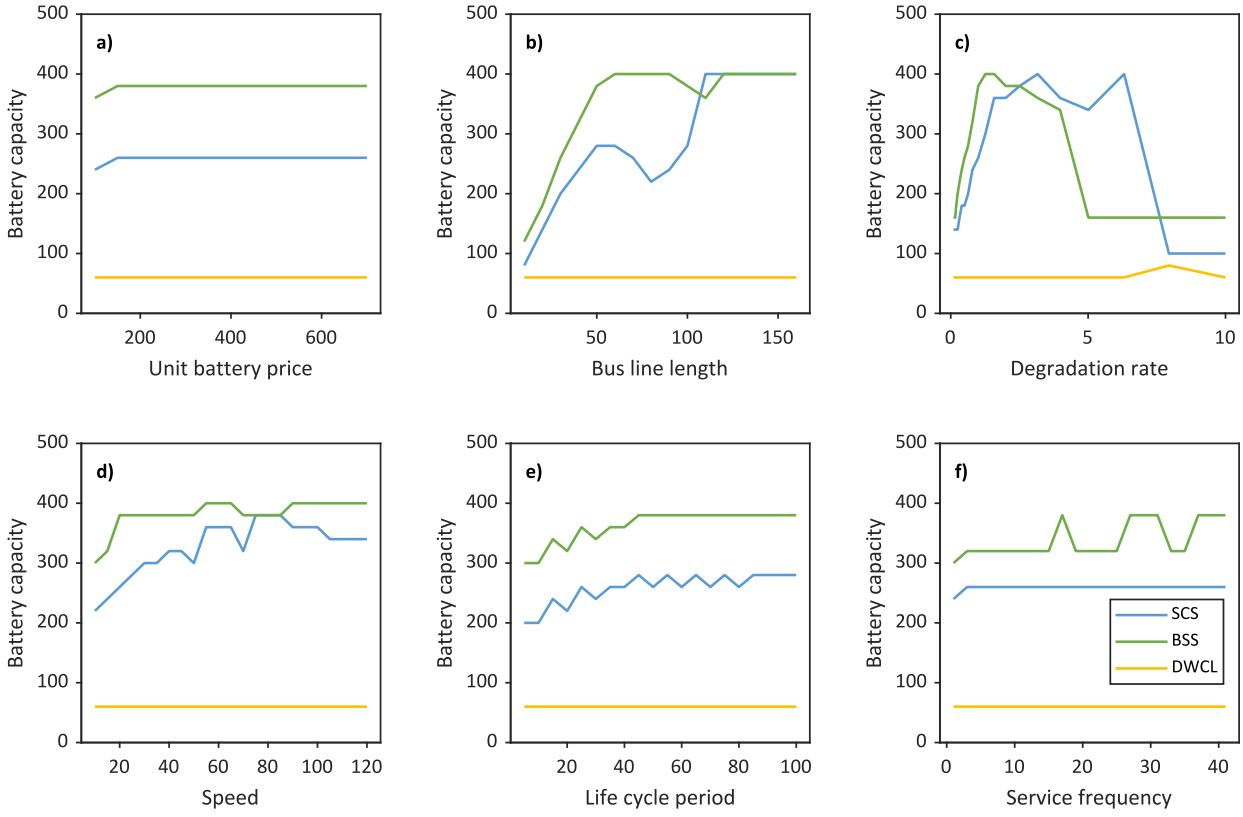

Fig. 11. Sensitivity of battery capacity to (a) unit battery price ($/kWh); (b) bus line length (km); (c) degradation rate; (d) speed (km/h); (e) life cycle period (year); and (f) service frequency (veh/h).

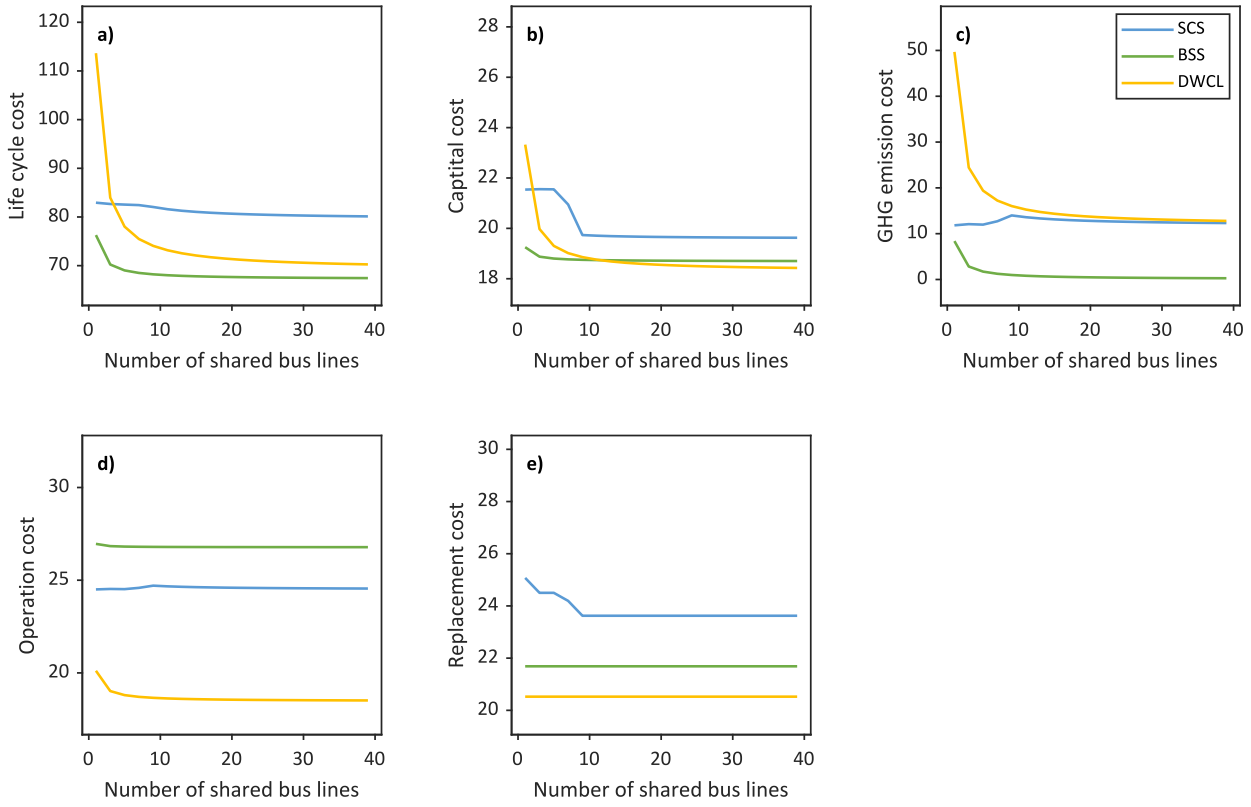

Fig. 12. Performance with varying numbers of shared bus lines; (a) Life cycle cost (million $); (b) capital cost (million $); (c) GHG emission cost (million $); (d) operating cost (million $); (e) replacement cost (million $).

the SCS system. When the DWCL is further reduced to less than 15 %, the DWCL is the most competitive choice. Specifically, the capital costs of the SCS and DWCL systems decrease as the systems are shared with more private cars because the capital cost, especially the construction cost of charging stations, is shared. Fig. 13(c) shows that the increasing penetration of private cars significantly reduces GHG emission costs, especially for DWCLs, since the emission costs for the charging infrastructure are shared by private cars. The maintenance costs of the DWCL system decrease with an increasing percentage of private cars, as shown in Fig. 13(d). The replacement costs of batteries and buses minimally change when charging stations are shared with private cars, as shown in Fig. 13(e).

5.3. *Worldwide application*

To evaluate the proposed LCC competitiveness analysis method for different e-bus transit systems, we apply to the approach to 38 BRT cities and their corridor operation data from the Institute of Transportation & Development Policy (ITDP) website, as shown in Fig. 14. Using the proposed models, the most competitive e-bus transit system for each city is selected based on real-world operating data, and the results are presented in Table 8.

As shown in Table 8, the specific factors considered in the analysis of the most cost-effective or environmentally competitive e-bus transit system for each city include the BRT circuit length, service frequency, speed, number of lines in shared corridors, and number of BRT stations. However, it is worth emphasizing that various parameters, as demonstrated in Table 7, can be tailored to each city's specific requirements and seamlessly integrated into our model framework to derive optimal decisions. Table 8 shows that the BSS system generally results in the lowest LCC when the circuit length is short. For long circuit lengths and high service frequencies, the DWCL system is the most competitive option. In particular, in the city of Jakarta, which has a very long circuit length, the SCS system is preferred. Compared to the service frequency, the circuit length has a more pronounced impact on the selection of the most competitive system.

When considering a shared charging infrastructure with buses and private cars, e.g., 10 % buses and 90 % cars, the most cost-competitive option changes from BSS to DWCL for some cities with moderate-range bus lines and not exceptionally high service frequencies. After considering shared charging infrastructure in all cities, the cities in which the BSS system remains the most cost-competitive tend to have short bus line lengths and low service frequencies. This is because the BSS system adequately fulfills the local operational requirements, reducing the demand for constructing expensive wireless charging infrastructure and avoiding the high costs of battery purchases, degradation, and replacement.

In addition, the BSS and SCS systems are more cost competitive in the context of reducing GHG emissions since the DWCL system

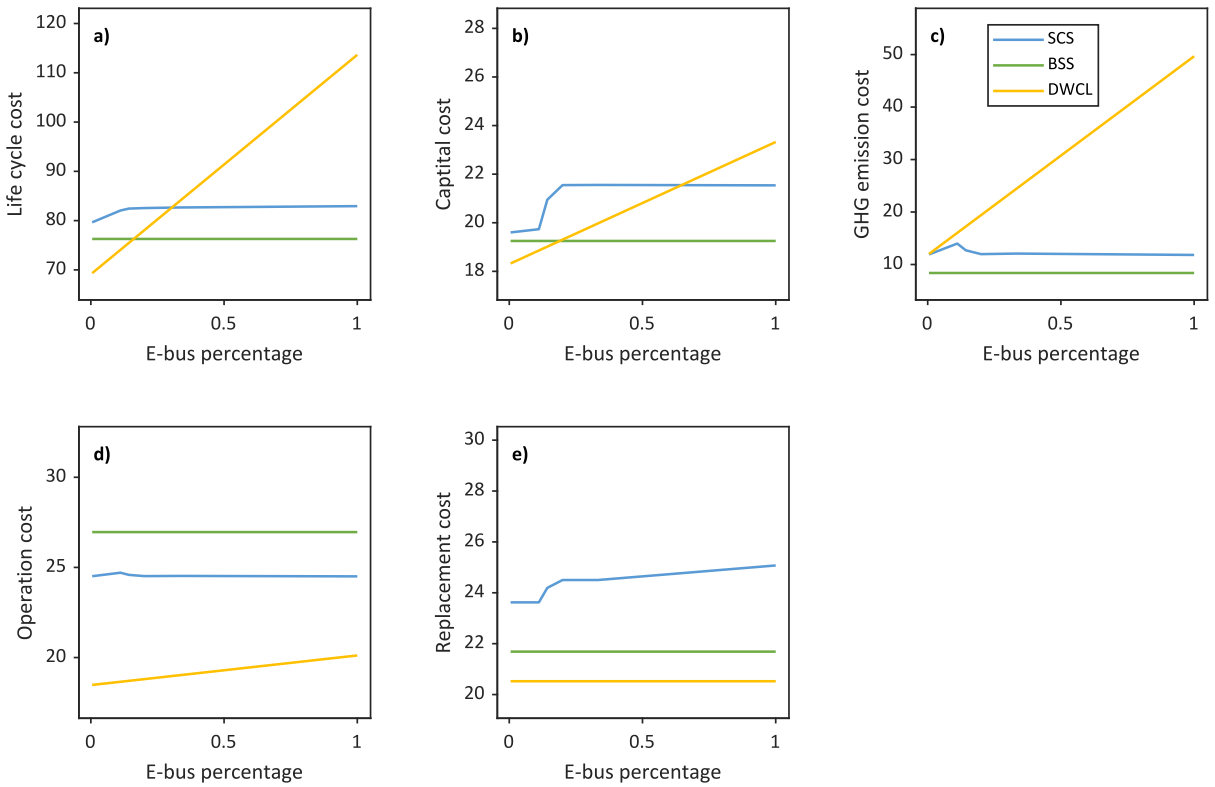

Fig. 13. Cost performance of e-bus charging infrastructure systems with varying e-bus percentages. (a) Life cycle cost (million $); (b) capital cost (million $); (c) GHG emission cost (million $); (d) operating cost (million $); (e) replacement cost (million $).

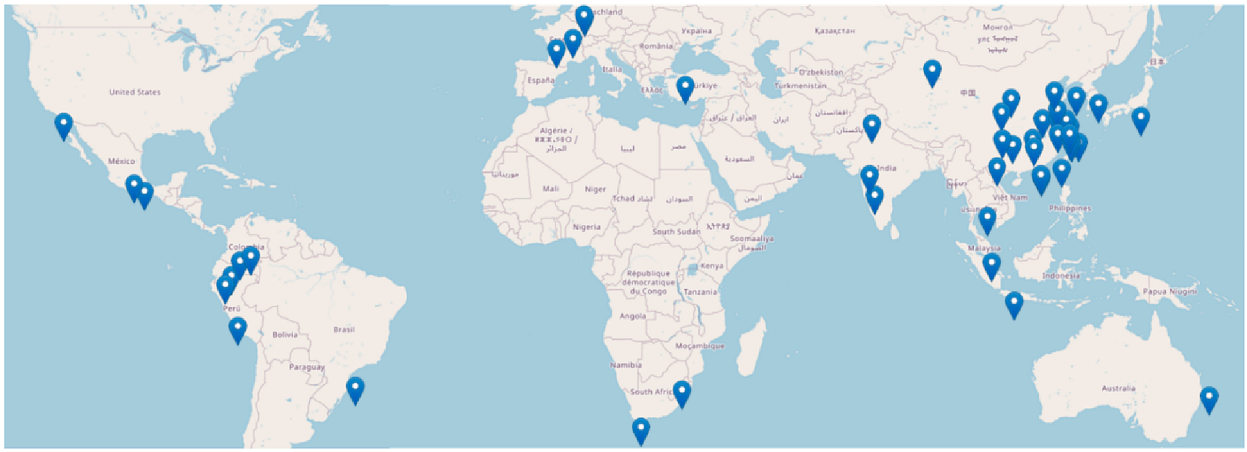

Fig. 14. 38 BRT cities and their locations (Website: https://www.itdp.org/).

produces more air pollution during construction and has lower efficiency during wireless power transfer.

6. Conclusions

Electric bus transit systems play an essential role in e-mobility for sustainable transportation, and their contributions to improved energy efficiency and sustainability heavily rely on the deployed batteries and charging infrastructure. In this work, a modeling and optimization framework is developed to analyze the LCC and environmental effects of e-bus transit systems equipped with different charging devices. For each type of transit system, key design parameters, e.g., the fleet size, battery capacity, and length of charging lanes, are optimally selected, and cost competitiveness is quantitatively analyzed.

Table 8
BRT corridors and their corresponding most competitive e-bus transit systems.

City	Circuit length (km)	Service frequency (veh/h)	Speed (km/h)	Number of lines in shared corridors	Number of BRT stations	Most competitive e-bus transit system (No shared)	Most competitive e-bus transit system (LCC for 100 %, 10 %, and 1 % buses)			Most competitive e-bus transit system (GHG cost for 100 %, 10 %, and 1 % buses)		
Amsterdam	56.7	18	34	4	33	BSS	BSS	DWCL	DWCL	BSS	BSS	BSS
Bangkok	15.3	15	28	1	12	BSS	BSS	BSS	BSS	BSS	BSS	BSS
Beijing	79	18	17.8	5	78	BSS	BSS	DWCL	DWCL	BSS	BSS	BSS
Bogota	108	312	30	108	142	DWCL	DWCL	DWCL	DWCL	BSS	BSS	BSS
Brisbane	28.7	232	25	150	26	BSS	BSS	BSS	BSS	BSS	BSS	BSS
Buenos Aires	64.1	193	23.6	71	122	DWCL	DWCL	DWCL	DWCL	BSS	BSS	BSS
Cali	35.6	164	14.5	10	58	BSS	BSS	DWCL	DWCL	BSS	BSS	BSS
Changde	18.9	27	31	8	24	BSS	BSS	BSS	BSS	BSS	BSS	BSS
Changzhou	54	43	17	13	59	DWCL	DWCL	DWCL	DWCL	BSS	BSS	BSS
Chengdu	46.3	101	30	8	44	DWCL	DWCL	DWCL	DWCL	BSS	BSS	BSS
Dalian	13.7	86	19.3	3	11	BSS	BSS	BSS	BSS	BSS	BSS	BSS
Guangzhou	45	12	18	44	52	BSS	BSS	DWCL	DWCL	BSS	BSS	BSS
Hangzhou	55.4	67	12.23	50	76	BSS	BSS	DWCL	DWCL	BSS	BSS	BSS
Hefei	7.2	80	17	6	9	BSS	BSS	BSS	BSS	BSS	BSS	BSS
Istanbul	51.7	137	35	3	44	DWCL	DWCL	DWCL	DWCL	BSS	BSS	BSS
Jakarta	134	40	25	26	210	SCS	SCS	DWCL	DWCL	BSS	BSS	BSS
Jinan	41.6	49	17.5	5	56	BSS	BSS	DWCL	DWCL	BSS	BSS	BSS
Kuala Lumpur	5.3	16	21.1	1	7	BSS	BSS	BSS	BSS	BSS	BSS	BSS
Lanzhou	12.3	90	22	6	19	BSS	BSS	BSS	BSS	BSS	BSS	BSS
Leon	30.5	20	19	5	65	BSS	BSS	BSS	BSS	BSS	BSS	BSS
Lianyungang	34	25	18	8	29	BSS	BSS	BSS	BSS	BSS	BSS	BSS
Lima	27.1	220	20.64	6	38	BSS	BSS	BSS	BSS	BSS	BSS	BSS
Los Angeles	30.8	16	32	3	18	BSS	BSS	BSS	BSS	BSS	BSS	BSS
Mexico City	81.5	56	18	8	115	DWCL	DWCL	DWCL	DWCL	BSS	BSS	BSS
Nagoya	6.7	12	25	4	9	BSS	BSS	BSS	BSS	BSS	BSS	BSS
Nanning	28.5	51	15.37	28	31	BSS	BSS	BSS	BSS	BSS	BSS	BSS
Nantes	6.6	9	19	1	15	BSS	BSS	BSS	BSS	BSS	BSS	BSS
Seoul	44.4	210	20	45	73	BSS	BSS	DWCL	DWCL	BSS	BSS	BSS
Shaoxing	19	15	15	1	12	BSS	BSS	BSS	BSS	BSS	BSS	BSS
Urumqi	51.2	93	13	9	58	DWCL	DWCL	DWCL	DWCL	BSS	BSS	BSS
Xiamen	53.18	53	31.6	6	42	BSS	BSS	DWCL	DWCL	BSS	BSS	BSS
Yancheng	16	39	18	8	25	BSS	BSS	BSS	BSS	BSS	BSS	BSS
Yichang	21	94	20	2	22	BSS	BSS	BSS	BSS	BSS	BSS	BSS
Yinchuan	21	44	17.2	10	22	BSS	BSS	BSS	BSS	BSS	BSS	BSS
Zaozhuang	65	23	28	8	56	BSS	BSS	DWCL	DWCL	BSS	BSS	BSS
Zhengzhou	115.5	129	17	31	136	DWCL	DWCL	DWCL	DWCL	BSS	BSS	BSS
Zhongshan	13	26	24	5	13	BSS	BSS	BSS	BSS	BSS	BSS	BSS
Zhoushan	23	47	19	1	10	BSS	BSS	BSS	BSS	BSS	BSS	BSS

Note: (1) All BRT data are from the Institute of Transportation & Development Policy (ITDP) website.
(2) Service frequency and operating speed data correspond to peak hours since data for off-peak hours are lacking.

With the city of Guangzhou in China as a case study, the costs of different systems were calculated, and sensitivity analyses were performed for various parameter values. For instance, the BSS system was determined to be superior to the other systems, and its cost was most sensitive to battery degradation. SCS systems demonstrate better competitiveness when the bus line length is very long. Then, by applying the developed analysis framework to BRTs in 38 cities worldwide, we found that the most cost-competitive options varied among these cities due to various factors, e.g., different circuit lengths and service frequencies. In addition, the preferred system option may change with the percentage of private cars shared.

From a comprehensive life-cycle perspective, this study provides the most cost-competitive options for e-bus transit systems along with optimal design parameter values. Furthermore, the proposed optimization and sensitivity analysis framework can provide valuable insights for policymakers in terms of economic cost and environmental impact. For instance, when selecting and designing an e-bus transit system, policymakers should consider multiple factors, such as bus line length, service frequency, and the number of shared bus lines. In particular, the proposed modeling and optimization framework can be universally applied to various cities, and it might yield different e-bus transit system options depending on the specific e-bus route characteristics of a given city.

While this study provides valuable insights into the planning and design of e-bus transit systems, it still has several limitations. Due to various assumptions and simplifications, though necessary for tractability, the developed e-bus transit system models cannot fully capture the diversity of system and city characteristics in practice. For instance, the assumption of a uniform battery size for each e-bus renders the model unsuitable for practical e-buses equipped with different battery types or sizes. Moreover, some real-world concerns, such as time-varying electricity costs, uncertainty in energy consumption, unpredictable technological advancements in batteries, and

various battery charging strategies, were not considered when modeling the system, thus limiting the applicability of the proposed method. The above limitations may be addressed in our future research, and cost and environmental analyses of the nexus between BRTs and power grids will be investigated. Moreover, more complex traffic systems with autonomous vehicles, ridesharing, and modular buses will be explored.

CRediT authorship contribution statement

Mingyang Pei: Conceptualization, Methodology, Software, Writing – original draft. **Yi Hu:** Formal analysis, Methodology, Software, Writing – original draft. **Weiji Han:** Supervision, Validation, Writing – review & editing. **Xiaobo Qu:** Project administration, Supervision, Validation. **Changfu Zou:** Project administration, Supervision, Validation, Writing – review & editing.

Declaration of competing interest

The authors declare that they have no known competing financial interests or personal relationships that could have appeared to influence the work reported in this paper.

Acknowledgments

This work was supported in part by the Transport Area of Advance at the Chalmers University of Technology and in part by the Guangzhou Basic and Applied Basic Research (SL2023A04J00802), and the Science and Technology Commission of Shanghai Municipality (23160713400).

Appendix

APPENDIX A. GHG EMISSION FACTORS FOR LCC ANALYSIS.

Table 9. GHG emission factors for LCC analysis.

	Item	Notation	Unit	GHG CO_2
Dynamic wireless charging lane	Pavement	a_{pav}	kg/m^2	1630.00
	Underground feeder	a_{feeder}	kg/km	111503.70
	Connecting wire	a_{wire}	kg/km	25.00
	Inverter	a_{inv}	kg/piece	12800.00
	Transformer	a_{trans}	kg/piece	6060.00
	Coil transmitter (6 KW)	a_{coil}	kg/piece	453.00
Swapping station	Construction area	a_{con}	kg/m^2	2930.00
	Chargers	a_{char}	piece	3000.00
	Connecting wire	a_{wire}	kg/km	25.00
	Inverter	a_{inv}	kg/piece	12800.00
	Transformer	a_{trans}	kg/piece	6060.00
End-terminal station	Construction area	a_{con}	kg/m^2	2930.00
	Chargers	a_{char}	kg/piece	14000.00
	Connecting wire	a_{wire}	kg/km	25.00
	Inverter	a_{inv}	kg/piece	12800.00
	Transformer	a_{trans}	kg/piece	6060.00
Opportunity charging (plug-in)	Construction area	a_{con}	kg/m^2	2930.00
	Chargers	a_{char}	kg/piece	14000.00
	Connecting wire	a_{wire}	kg/km	25.00
	Inverter	a_{inv}	kg/piece	12800.00
	Transformer	a_{trans}	kg/piece	6060.00
Bus	Well-to-tank (WTT)	a_{WTT}	kg/km	0.02
	Tank-to-wheel (TTW)	–	–	–
	Glider	a_{ELC}	kg/km	0.035
	Powertrain		kg/kWh	170.00

Note: According to the definition in the Kyoto Protocol to the United Nations Framework Convention on Climate Change (UNFCCC), GHGs include six types of gas (Gerden, 2018), namely, carbon dioxide (CO2), methane (CH4), nitrous oxide (N2O), hydrofluorocarbons (HFCs), perfluorocarbons (PFCs) and sulfur hexafluoride (SF6). Since CH4, N2O, HFC, PFC and SF6 data are not commonly available for all life cycle periods, this work focused only on CO2. The method can be extended when we obtain data for other types of gases.

References

ABB Group, 2021. Electric Vehicle Infrastructure: Overnight charging for electric buses and trucks. ABB EV Infrastructure.

Adler, J.D., Mirchandani, P.B., 2014. Online routing and battery reservations for electric vehicles with swappable batteries. Transportation Research Part b: Methodological 70, 285–302. https://doi.org/10.1016/j.trb.2014.09.005.

Ahmad, A., Alam, M.S., Chabaan, R., 2017. A Comprehensive Review of Wireless Charging Technologies for Electric Vehicles. IEEE Transactions on Transportation Electrification 4, 38–63. https://doi.org/10.1109/TTE.2017.2771619.

An, K., Jing, W., Kim, I., 2020. Battery-swapping facility planning for electric buses with local charging systems. International Journal of Sustainable Transportation 14, 489–502. https://doi.org/10.1080/15568318.2019.1573939.

Andersson, M., 2017. Energy storage solutions for electric bus fast charging stations. Energy Systems Engineering at Uppsala University.

Bi, Z., Song, L., De Kleine, R., Mi, C.C., Keoleian, G.A., 2015. Plug-in vs. wireless charging: Life cycle energy and greenhouse gas emissions for an electric bus system. Applied Energy 146, 11–19. https://doi.org/10.1016/j.apenergy.2015.02.031.

Bi, Z., Kan, T., Mi, C.C., Zhang, Y., Zhao, Z., Keoleian, G.A., 2016. A review of wireless power transfer for electric vehicles: Prospects to enhance sustainable mobility. Applied Energy 179, 413–425. https://doi.org/10.1016/j.apenergy.2016.07.003.

Bi, Z., De Kleine, R., Keoleian, G.A., 2017. Integrated Life Cycle Assessment and Life Cycle Cost Model for Comparing Plug-in versus Wireless Charging for an Electric Bus System. Journal of Industrial Ecology 21, 344–355. https://doi.org/10.1111/jiec.12419.

Bi, Z., Keoleian, G.A., Lin, Z., Moore, M.R., Chen, K., Song, L., Zhao, Z., 2019. Life cycle assessment and tempo-spatial optimization of deploying dynamic wireless charging technology for electric cars. Transportation Research Part c: Emerging Technologies 100, 53–67. https://doi.org/10.1016/j.trc.2019.01.002.

BloombergNEF, 2020. Battery Pack Prices Cited Below $100/kWh for the First Time in 2020, While Market Average Sits at $137/kWh.

Borén, S., 2020. Electric buses' sustainability effects, noise, energy use, and costs. International Journal of Sustainable Transportation 14, 956–971. https://doi.org/10.1080/15568318.2019.1666324.

Charging, A.H., 2010. Electric Vehicle Infrastructure Overnight charging for electric buses and trucks.

Chatzikomis, C.I., Spentzas, K.N., Mamalis, A.G., 2014. Environmental and economic effects of widespread introduction of electric vehicles in Greece. European Transport Research Review 6, 365–376.

Chen, Z., Liu, W., Yin, Y., 2017. Deployment of stationary and dynamic charging infrastructure for electric vehicles along traffic corridors. Transportation Research Part c: Emerging Technologies 77, 185–206. https://doi.org/10.1016/j.trc.2017.01.021.

Chen, Z., Yin, Y., Song, Z., 2018. A cost-competitiveness analysis of charging infrastructure for electric bus operations. Transportation Research Part c: Emerging Technologies 93, 351–366. https://doi.org/10.1016/j.trc.2018.06.006.

Chesky,, 2021. Hybrid truck and blue electric car on wireless charging lane. Shutterstock.

Co, A.E., 2021. Matrix series embedded IoT Gateway make the management system at electric bus charging station more perfect. Artila Enbedded Networking and Computing.

European Commission, 2021. Fit for 55 - Delivering the EU's 2030 Climate Target on the way to climate neutrality.

Department of Transportation, 2021. FACT SHEET : Biden Administration Advances Electric Vehicle Charging Infrastructure.

European Environment Agency, 2020. National emissions reported to the UNFCCC and to the EU Greenhouse Gas Monitoring Mechanism. http://www.eea.europa.eu/data-and-maps/data/national-emissions-reported-to-the-unfccc-and-to-the-eu-greenhouse-gas-monitoring-mechanism-7.

Fuller, M., 2016. Wireless charging in California: Range, recharge, and vehicle electrification. Transportation Research Part c: Emerging Technologies 67, 343–356. https://doi.org/10.1016/j.trc.2016.02.013.

García, A., Monsalve-Serrano, J., Lago Sari, R., Tripathi, S., 2022. Life cycle CO_2 footprint reduction comparison of hybrid and electric buses for bus transit networks. Applied Energy 308, 118354. https://doi.org/10.1016/j.apenergy.2021.118354.

Gerden, T., 2018. The adoption of the kyoto protocol of t he united nations framework convention on climate change. Prispevki Za Novejso Zgodovino 58, 160–189. https://doi.org/10.51663/pnz.58.2.07.

Gong, L., Xiao, C., Cao, B., Zhou, Y., 2018. Adaptive Smart Control Method for Electric Vehicle Wireless Charging System. Energies 11. https://doi.org/10.3390/en11102685.

Guangzhou Bus Group, 2022. Guangzhou Bus Group Nansha Bus Co., Ltd. 30 sets of pure electric city bus procurement project bid announcement. Guangzhou.

Hassold, S., Ceder, A.A., 2014. Public transport vehicle scheduling featuring multiple vehicle types. Transportation Research Part b: Methodological 67, 129–143. https://doi.org/10.1016/j.trb.2014.04.009.

He, J., Yang, H., Tang, T.Q., Huang, H.J., 2020. Optimal deployment of wireless charging lanes considering their adverse effect on road capacity. Transportation Research Part c: Emerging Technologies 111, 171–184. https://doi.org/10.1016/j.trc.2019.12.012.

He, F., Yin, Y., Zhou, J., 2013. Integrated pricing of roads and electricity enabled by wireless power transfer. Transportation Research Part c: Emerging Technologies 34, 1–15. https://doi.org/10.1016/j.trc.2013.05.005.

Jagdishsingh, R., Patil, S., R.,, 2014. Life Cycle Costing Method. IOSR Journal of Mechanical and Civil Engineering 11, 01–05. https://doi.org/10.9790/1684-11220105.

Jang, Y.J., 2018. Survey of the operation and system study on wireless charging electric vehicle systems. Transportation Research Part c: Emerging Technologies 95, 844–866. https://doi.org/10.1016/j.trc.2018.04.006.

Jang, Y.J., Jeong, S., Lee, M.S., 2016. Initial energy logistics cost analysis for stationary, quasi-dynamic, & dynamicwireless charging public transportation systems. Energies 9. https://doi.org/10.3390/en9070483.

Johnson, C., 2020. Financial Analysis of Battery Electric Transit Buses 1–45.

Ji, J., Bie, Y., Zeng, Z., Wang, L., 2022. Trip energy consumption estimation for electric buses. Communications in Transportation Research 2, 100069. https://doi.org/10.1016/j.commtr.2022.100069.

Ke, B.R., Chung, C.Y., Chen, Y.C., 2016. Minimizing the costs of constructing an all plug-in electric bus transportation system: A case study in Penghu. Applied Energy 177, 649–660. https://doi.org/10.1016/j.apenergy.2016.05.152.

Kim, K.H., Han, Y.J., Lee, S., Cho, S.W., Lee, C., 2019. Text mining for patent analysis to forecast emerging technologies in wireless power transfer. Sustainability (switzerland) 11, 6240. https://doi.org/10.3390/su11226240.

Kpmg, 2021. Sinocharged: The bright future of China's electric vehicle market. The bright future of China's electric vehicle market, Sinocharged.

Lajunen, A., 2018. Lifecycle costs and charging requirements of electric buses with different charging methods. Journal of Cleaner Production 172, 56–67. https://doi.org/10.1016/j.jclepro.2017.10.066.

Lam, L., Bauer, P., 2013. Practical capacity fading model for Li-ion battery cells in electric vehicles. IEEE Transactions on Power Electronics 28, 5910–5918. https://doi.org/10.1109/TPEL.2012.2235083.

Lambert, F., 2018. The first 200-kW wireless charging system for electric buses is deployed. Electrek.

Lehmann, F., 2021. Electric city. TRATON.

Liang, X., Chowdhury, M.S.A., 2018. Emerging wireless charging systems for electric vehicles - Achieving high power transfer efficiency: A review, in: 2018 IEEE Industry Applications Society Annual Meeting, IAS 2018. Institute of Electrical and Electronics Engineers Inc. Doi: 10.1109/IAS.2018.8544484.

Liang, X., Zhang, S., Wu, Y., Xing, J., He, X., Zhang, K.M., Wang, S., Hao, J., 2019. Air quality and health benefits from fleet electrification in China. Nature Sustainability 2, 962–971. https://doi.org/10.1038/s41893-019-0398-8.

Liu, Z., Song, Z., 2017. Robust planning of dynamic wireless charging infrastructure for battery electric buses. Transportation Research Part c: Emerging Technologies 83, 77–103. https://doi.org/10.1016/j.trc.2017.07.013.

Liu, Y., Wang, L., Zeng, Z., Bie, Y., 2022. Optimal charging plan for electric bus considering time-of-day electricity tariff. Journal of Intelligent and Connected Vehicles 5, 123–137. https://doi.org/10.1108/JICV-04-2022-0008.

Liu, C., Wei, B., Wu, X., Wang, S., Xu, J., 2019. Engineering Application of Dynamic Wireless Charging Technology for Electric Vehicles. Dianwang Jishu/power System Technology 43, 2211–2218. https://doi.org/10.13335/j.1000-3673.pst.2018.2433.
Liu, T., (Avi) Ceder, A.,, 2020. Battery-electric transit vehicle scheduling with optimal number of stationary chargers. Transportation Research Part c: Emerging Technologies 114, 118–139. https://doi.org/10.1016/j.trc.2020.02.009.
Lukic, S., Pantic, Z., 2013. Cutting the Cord: Static and Dynamic Inductive Wireless Charging of Electric Vehicles. IEEE Electrification Magazine 1, 57–64. https://doi.org/10.1109/mele.2013.2273228.
Majhi, R.C., Ranjitkar, P., Sheng, M., Covic, G.A., Wilson, D.J., 2021. A systematic review of charging infrastructure location problem for electric vehicles. Transport Reviews 41, 432–455. https://doi.org/10.1080/01441647.2020.1854365.
Mak, H.Y., Rong, Y., Shen, Z.J.M., 2013. Infrastructure planning for electric vehicles with battery swapping. Management Science 59, 1557–1575. https://doi.org/10.1287/mnsc.1120.1672.
Manzolli, J.A., Trovão, J.P., Antunes, C.H., 2022. A review of electric bus vehicles research topics – Methods and trends. Renewable and Sustainable Energy Reviews 159. https://doi.org/10.1016/j.rser.2022.112211.
Messagie, M., 2017. Life Cycle Analysis of the Climate Impact of Electric Vehicles. Transport and Environment 14.
Mohamed, N., Aymen, F., Ben Hamed, M., Lassaad, S., 2020. Analysis of battery-EV state of charge for a dynamic wireless charging system. Energy Storage 2. https://doi.org/10.1002/est2.117.
Nie, Y., Ghamami, M., 2013. A corridor-centric approach to planning electric vehicle charging infrastructure. Transportation Research Part b: Methodological 57, 172–190. https://doi.org/10.1016/j.trb.2013.08.010.
Nordelöf, A., Messagie, M., Tillman, A.M., Ljunggren Söderman, M., Van Mierlo, J., 2014. Environmental impacts of hybrid, plug-in hybrid, and battery electric vehicles—what can we learn from life cycle assessment? International Journal of Life Cycle Assessment 19, 1866–1890. https://doi.org/10.1007/s11367-014-0788-0.
Nordelöf, A., Romare, M., Tivander, J., 2019. Life cycle assessment of city buses powered by electricity, hydrogenated vegetable oil or diesel. Transportation Research Part d: Transport and Environment 75, 211–222. https://doi.org/10.1016/j.trd.2019.08.019.
Olsen, N., Kliewer, N., 2022. Location Planning of Charging Stations for Electric Buses in Public Transport Considering Vehicle Scheduling: A Variable Neighborhood Search Based Approach. Applied Sciences (switzerland) 12. https://doi.org/10.3390/app12083855.
Panchal, C., Stegen, S., Lu, J., 2018. Review of static and dynamic wireless electric vehicle charging system. Engineering Science and Technology, an International Journal 21, 922–937. https://doi.org/10.1016/J.JESTCH.2018.06.015.
Pathak, A., Sethuraman, G., Ongel, A., Lienkamp, M., 2021. Impacts of electrification & automation of public bus transportation on sustainability—A case study in Singapore. Forschung Im Ingenieurwesen/engineering Research 85, 431–442. https://doi.org/10.1007/s10010-020-00408-z.
Pei, M., Lin, P., Du, J., Li, X., Chen, Z., 2021. Vehicle dispatching in modular transit networks: A mixed-integer nonlinear programming model. Transportation Research Part e: Logistics and Transportation Review 147, 102240. https://doi.org/10.1016/j.tre.2021.102240.
Pei, M., Zhu, H., Ling, J., Hu, Y., Yao, H., Zhong, L., 2023. Empowering highway network: Optimal deployment and strategy for dynamic wireless charging lanes. Communications in Transportation Research 3, 100106. https://doi.org/10.1016/j.commtr.2023.100106.
Qu, X., Wang, S., 2021. Communications in Transportation Research: Vision and scope. Communications in Transportation Research 1, 100001. https://doi.org/10.1016/j.commtr.2021.100001.
Ruan, T., Lv, Q., 2022. Public perception of electric vehicles on reddit over the past decade. Communications in Transportation Research 2, 100070. https://doi.org/10.1016/j.commtr.2022.100070fv.
Shi, X., Wang, Z., Li, X., Pei, M., 2021. The effect of ride experience on changing opinions toward autonomous vehicle safety. Communications in Transportation Research 1, 100003. https://doi.org/10.1016/j.commtr.2021.100003.
Sierzchula, W., Bakker, S., Maat, K., Van Wee, B., 2014. The influence of financial incentives and other socio-economic factors on electric vehicle adoption. Energy Policy 68, 183–194. https://doi.org/10.1016/j.enpol.2014.01.043.
Statista Research Department, 2021. Electricity prices for households in Sweden from 2010 to 2021, semi-annually [WWW Document]. Statista.
Statusrapport, 2020. Samarbete kring framtidens elektrifierade transporter.
Suomalainen, E., Colet, F., 2019. A corridor-based approach to estimating the costs of electric vehicle charging infrastructure on highways. World Electric Vehicle Journal 10. https://doi.org/10.3390/wevj10040068.
Volvo Bus Corporation, 2019.
Wang, Y., Lu, C., Bi, J., Sai, Q., Qu, X., 2022b. Lifecycle Cost Optimization for Electric Bus Systems With Different Charging Methods: Collaborative Optimization of Infrastructure Procurement and Fleet Scheduling. IEEE Transactions on Intelligent Transportation Systems PP, 1–20. Doi: 10.1109/TITS.2022.3223028.
Wang, Y., Liao, F., Lu, C., 2022a. Integrated optimization of charger deployment and fleet scheduling for battery electric buses. Transportation Research Part D 109, 103382. https://doi.org/10.1016/j.trd.2022.103382.
Wang, J., 2021. The number of social vehicles served by charging stations at bus stations in Guangzhou has increased by about 30%. Yangcheng Newspaper 3.
Woodward, D.G., 1997. Life cycle costing - Theory, information acquisition and application. International Journal of Project Management 15, 335–344. https://doi.org/10.1016/S0263-7863(96)00089-0.
XJ Group Corporation, 2021. Battery swapping for electric buses in Qingdao. PHOENIX CONTACT.
Xu, M., Wu, T., Tan, Z., 2021. Electric vehicle fleet size for carsharing services considering on-demand charging strategy and battery degradation. Transportation Research Part c: Emerging Technologies 127. https://doi.org/10.1016/j.trc.2021.103146.
Xylia, M., Leduc, S., Laurent, A.B., Patrizio, P., van der Meer, Y., Kraxner, F., Silveira, S., 2019. Impact of bus electrification on carbon emissions: The case of Stockholm. Journal of Cleaner Production 209, 74–87. https://doi.org/10.1016/j.jclepro.2018.10.085.
Yang, S., Yao, J., Kang, T., Zhu, X., 2014. Dynamic operation model of the battery swapping station for EV (electric vehicle) in electricity market. Energy 65, 544–549. https://doi.org/10.1016/j.energy.2013.11.010.
Zeng, Z., Qu, X., 2023. What's next for battery-electric bus charging systems. Communications in Transportation Research 3, 100094. https://doi.org/10.1016/j.commtr.2023.100094.
Zeng, Z., Wang, S., Qu, X., 2022. On the role of battery degradation in en-route charge scheduling for an electric bus system. Transportation Research Part e: Logistics and Transportation Review 161, 102727. https://doi.org/10.1016/j.tre.2022.102727.
Zhang, L., Han, Y., Peng, J., Wang, Y., 2023. Vehicle and Charging Scheduling of Electric Bus Fleets: A Comprehensive Review. Journal of Intelligent and Connected Vehicles 6, 116–124. https://doi.org/10.26599/JICV.2023.9210012.
Zhang, L., Zeng, Z., Gao, K., 2022. A bi-level optimization framework for charging station design problem considering heterogeneous charging modes. Journal of Intelligent and Connected Vehicles 5, 8–16. https://doi.org/10.1108/JICV-07-2021-0009.
Zhang, L., Zeng, Z., Qu, X., 2021. On the Role of Battery Capacity Fading Mechanism in the Lifecycle Cost of Electric Bus Fleet. IEEE Transactions on Intelligent Transportation Systems 22, 2371–2380. https://doi.org/10.1109/TITS.2020.3014097.
Zheng, Y., Dong, Z.Y., Xu, Y., Meng, K., Zhao, J.H., Qiu, J., 2014. Electric vehicle battery charging/swap stations in distribution systems: Comparison study and optimal planning. IEEE Transactions on Power Systems 29, 221–229. https://doi.org/10.1109/TPWRS.2013.2278852.
Zhong, L., Pei, M., 2020. Optimal design for a shared swap charging system considering the electric vehicle battery charging rate. Energies 13. https://doi.org/10.3390/en13051213.
Zhou, Y., Wang, H., Wang, Y., Li, R., 2022. Robust optimization for integrated planning of electric-bus charger deployment and charging scheduling. Transportation Research Part d: Transport and Environment 110, 103410. https://doi.org/10.1016/j.trd.2022.103410.